MethodsX 11 (2023) 102420

Contents lists available at ScienceDirect

MethodsX

journal homepage: www.elsevier.com/locate/methodsx

# Methodologies for modeling and identification of breathing crack: A review

Sayandip Ganguly

*Indian Institute of Technology, Patna 801103, India*

## REVIEW HIGHLIGHTS

- The mathematical connection is reviewed between the Volterra series and other nonlinear system identification techniques.
- Methods developed for the identification of breathing cracks using its nonlinear behavior are summarized.
- Experimental models developed for nonlinear system identification techniques are explored to evaluate their potential for the simulation of breathing crack mechanism.

## ARTICLE INFO

*Method name:*
*Volterra series, higher order frequency response function, nonlinear output frequency response function, general frequency response function, output frequency response function, perturbation method, harmonic balance method, acoustic methods, vibro-acoustic methods*

*Keywords:*
Structural health monitoring
Breathing crack
Nonlinearity
Damage indicator

## ABSTRACT

Swift development of technology for monitoring complex structures demands major attention on the precision of damage detection methods. The early detection of any type of deterioration or degradation of structures is of paramount importance to avoid sudden catastrophic failure. It warns users about the impending state of the system. At the initiation of a crack or some other system faults, the system may generate a time-varying state of crack under ambient vibration. It represents the nonlinear breathing phenomena of crack. An assessment of this degree of nonlinearity can be utilized for the detection, localization, and quantification of breathing cracks. Appropriate modeling of such cracks is thus necessary to capture distinctive nonlinear features. Recognizing this importance, various methods of modeling and nonlinear system identification which have been employed in the past for the detection of breathing crack are reviewed. The present study also explores some of the available vibration as well as acoustic-based damage identification techniques, chronologically connecting their evolutions. It summarizes the advantages and limitations of the methods to inspect potential future applications. The future scopes drawn from this review are highlighted to pave the path of wide-spread applications of nonlinear features of crack.

## Specifications table

| | |
|---|---|
| Subject area: | Engineering |
| More specific subject area: | *Structural Health Monitoring* |
| Name of the reviewed methodology: | *Volterra series, higher order frequency response function, nonlinear output frequency response function, general frequency response function, output frequency response function, perturbation method, harmonic balance method, acoustic methods, vibro-acoustic methods* |
| Keywords: | *Structural health monitoring; Breathing crack; Nonlinearity; Damage indicator* |
| Resource availability: | *NA* |

(*continued on next page*)

*E-mail address:* sayandip_2021ce19@iitp.ac.in

https://doi.org/10.1016/j.mex.2023.102420
Received 1 February 2023; Accepted 6 October 2023
Available online 11 October 2023

Review question:

1. *How to apply nonlinear system identification techniques to detect presence of breathing crack in a system and its nonlinear behavior*
2. *What are the advantages and limitations of different classical methods evolved for the solution of nonlinear equation*
3. *Which methods among numerical and theoretical solution techniques perform better in capturing actual nonlinear phenomena of a system*
4. *How nonlinear damage indicator is related to bispectrum and bicoherence analysis in detection of breathing crack*
5. *What are the different analytical and numerical procedures available to precisely simulate behavior of breathing crack*
6. *What are the limitations of different experimental models developed to simulate breathing behavior of crack and validate damage indicators' performance*

## Method details

### Background

Operational environment of a structure may cause rapid degradation in the performance as well as the design life-span. Timely monitoring is an important task to maintain safety, serviceability, and design life of the structure. Earlier, some in-situ non-destructive tests were considered as one of the reliable solutions for monitoring a structure. However, to detect an internal or sub-surface flaw of relatively small size in a complex structure by these methods is a strenuous job. Perceiving this constraint, the past decades have been marked by a significant increase in research interest on the evaluation of various damage detection methods. Most of such methods developed till days for monitoring structures are based on linear assumptions [1]. It may mislead the identification of crack initiation at its incipient state. Apparently, a small crack seems to have insignificant effect on the response and could not be identified by the minimal changes in linear response parameters. With frequent cyclic or fatigue loading, a crack from its embryonic state may grow up to severe state within a small time-frame. Thus, detection of crack even at an early state is a priority now-a-days. It prevents the growth of crack as well as mitigate the risk of collapse by optimizing maintenance of structure. The dire need for fatigue crack detection can also be gauged by the derailment of a Norfolk Southern train that happened in the United States on 11th July 2012. After a thorough investigation [2], it was revealed that several fatigue damages occurred on the surface of rail by moving load of train caused the fracture of section and consequently led to such incident. An early detection of fatigue crack by its nonlinear characteristics could have prevented such a tragic incident. The cost involved in repairing severe damage that may have grown gradually from a small crack can be reduced if the initiation of the crack can be identified in advance. A structure that behaves linearly in its healthy state, may exhibit nonlinear characteristics with the appearance of small cracks. Several past studies [3] have concluded that the sensitivity of nonlinear parameters is prominent even at small damage with time varying states of crack. Generation of higher harmonics, shift of resonance frequency are some of the sensitive nonlinear features that indicate presence of damage or degradation of material. A fully open model of crack is unable to represent these features. Consideration of nonlinear features of breathing cracks or crack modulated guided waves enhances early damage detection capability. It in turn safeguards the member against sudden collapse as well as rings the alarm about faulty members. There may also co-exist many other sources of nonlinearity. Material properties, loose fixity of joint, etc. are among those which also produce nonlinearity in the response. Extraction of only damage-sensitive features from the response is thus an exigent task in the detection of fatigue cracks. Before a detailed review, evolution of vibration, acoustic, and vibro-acoustic based methods originated for early detection of breathing crack is briefly outlined here.

The effect of local cracks on the vibration characteristics is first studied by Kirmsher [4] in 1944. The theoretical background of the vibration characteristics of a cracked shaft is then developed by Dimarogonas [5]. Pafelias [6] with the knowledge of vibrational property of a cracked shaft and extensive experimental analysis, proposed the concept of harmonic generation in presence of a crack. A few years later, generation of superharmonics by an external compressive-stretching cycle between two unbonded surfaces is experimentally investigated by Buck et al. [7]. Afterward, most of the research conducted on dynamic analysis of closing crack considered this phenomenon as a basic nonlinear feature. Tsyfansky and Beresnevich [8] studied the sensitivity of natural frequency to damage induced changes. A minimum deviation of 1 % to 1.5 % in natural frequency is observed when crack spreads over 15 %–20 % area of the cross-section of a member. Several studies based on natural frequency and mode shape performed at this time are lacking to precisely identify small cracks due to their low sensitivity to damage. Detection of the most sensitive damage feature that affects response of a structure with real crack scenarios is yet to be unveiled. An effort is also made to mathematically express the response obtained from the system in presence of nonlinear crack. Mild crack with minimum degree of nonlinearity is attempted to solve by the application of perturbation technique. For strongly nonlinear system an exact long-term solution is difficult to predict by this method. Maezawa et al. in 1980 [9] demonstrated a possible closed-form solution for an un-symmetric piecewise-linear system subjected to a periodic response. Fourier series expansion with appropriate coefficients is employed to obtain steady-state solution of a single degree-of-freedom (DoF) system with two distinct boundary conditions. The convergence of the solution is further improved by series transformation for the analysis of higher-order harmonics [10]. The assumed solution procedures require exact time of contact of two cracked surfaces; deviation of which may result increased uncertainty in the solution . It also couldn't incorporate every type of nonlinear feature in the predicted solution. Satio [11] in 1985, used a complex form of variable and fast Fourier transformation (FFT) for the solution of vibration response of Jeffcott model. Subharmonic phenomenon is not included in this solution. Drawbacks of these solutions are addressed in the work of Choi and Noah [12] by using harmonic balance Newton-Raphson method along with FFT algorithm. The solution of nonlinear equations by this method shows that the occurrence of superharmonic resonance is limited to

some specific range of frequency. Subharmonic resonant frequency is also evaluated by this method. In another study, the probability of the detection of closing crack and the reliability of measured crack size are experimented by Clark et al. [13] with different testing procedures. Both magnetic particle inspection (MPI) and alternating current field measurement (ACFM) non-destructive techniques exhibited 100 % reliability in predicting crack length with ±10 % variations during opening and closing of crack. On the other hand, dye penetration and Rayleigh wave failed to determine the crack length in the closing cycle with a fair amount of reliability. The formulation of advanced methods for the localization and estimation of breathing crack depth has been taken up in numerous research following previous works [14–16]. However, the nature of nonlinear vibration makes it difficult to develop a single methodology for all types of problems. The characteristics of nonlinear vibration for different range of parameters of the system is still being investigated to find either a common solution technique or a damage-sensitive feature [17–20].

Advancement in various nonlinear system identification techniques also extended its application area to detection of cracks with nonlinear characteristics. A detailed discussion on various nonlinear system identification techniques has been presented in a review by Kerschen et al. [21]. Peng et al. in 2007 [22] introduced nonlinear output frequency response function (NOFRF) to detect the presence of cracks and investigated the impact of the crack size on different frequency peaks. Precise estimation of nonlinear response is the main constraint for the successful application of damage indicators developed in the past. Investigation on the development of advanced nonlinear solution procedures is also simultaneously grown at this time. Chatterjee [23] in 2010 applied Volterra series for the analysis of nonlinear response of a cantilever beam with a fatigue crack. In this work, nonlinear mechanism of fatigue crack is modeled by considering the system as bilinear oscillator. Bilinear restoring force is expressed in the form of a polynomial series for this system. The crack size is then measured quantitatively by comparing amplitudes of first and second harmonic responses. The effect of crack location and depth on the fundamental frequency of a beam is investigated in the work of Rezaee and Hassannejad [24]. Simplicity of linear equations for each region in bilinear oscillator is utilized by Yan et al. [25] to solve the breathing crack induced bi-linear stiffness. Natural frequency for each stiffness region is separately estimated and compared. The change in natural frequency in each region indicates the presence of breathing crack which is further employed for quantitative measurement of the crack. Bifurcation diagram, distortion of phase space, and Poincaré map are other indicators of nonlinear systems. Hence, these indicators have also been exercised in various works to extract unique features of breathing cracks [26,27].

Modulation of a propagating waveform by the interference of a crack is also proved to be superior in the detection and characterization of fatigue crack. In the early 1960, ultrasonic waves were majorly employed to detect material nonlinearity. The nonlinear features of wave interaction with crack such as scattering or reflection of wave, generation of higher harmonics are evolved gradually for the identification of micro crack in different structures such as plate, cylindrical shell etc. Richardson [28] analytically computed efficiency of second harmonic generation in presence of nonlinear crack. It is described as a function of the ratio of ambient hydrostatic pressure to the maximum compressive stress amplitude of the incident wave. Later, in 1993 Shan and Dewhurst [29] applied the modulation of ultrasonic wave to detect surface crack. Solodov et al. [30] discovered some “nonclassical” effects generated by the interaction between high-frequency nonlinear acoustic wave and asymmetrically varied stiffness characteristics of crack as a feature of contact acoustic nonlinearity (CAN). Interaction of fatigue crack adjacent to a fastener hole and Lamb wave propagated through the wave guide is studied by Cho and Lissenden [31]. An effort is made to establish a relation between damage severity and transmission coefficient ratio. Shen and Giurgiutiu [32] in 2014 formulated a predictive solution technique with two modeling approaches for crack-wave interaction. The generation of second harmonic as a signature of nonlinear wave interaction is also validated in this work with analytical solution. In 2018, to understand the nonlinear phenomenon developed by crack-wave interaction, CAN is analytically scrutinized by Wang et al. [33] and a reference free nonlinear index is proposed to correlate crack parameters with wave-embodied nonlinear characteristics. At the same time, by capturing scattered wave generated at the break-surface of a two-dimensional waveguide, orientation and depth of crack are measured by Wang et al. [34]. Till date, most of the approaches assumed to numerically simulate breathing behavior of crack are computationally challenging. One year later in 2019, Shen and Cesnik [35] numerically simulates nonlinear pattern developed by the interaction of Lamb wave and breathing crack with a local interaction simulation approach. A notable result is achieved in terms of computational efficiency with the adoption of this method. With more improvement, three-dimensional (3D) fatigue crack modeling approach is proposed by Xu et al. [36] in 2021 for the study of model driven growth prediction. An analytical solution to estimate second harmonic amplitude of lamb wave is also developed by Xu et al. [37]. Afterward, in a recent study (2022), Xu et al. [38] investigated scattered Rayleigh wave for surface/sub surface crack estimation. A closed-form expression for displacement magnitude of second harmonic in both surface or subsurface crack conditions is formulated by applying second equivalent stress component of decomposed Rayleigh wave at the crack surface.

With the advancement of technology and signal processing tools, sensitivity of guided wave unfolded as one of the promising technology to detect breathing crack or micro-crack. However, practical application and interpretation of ultrasonic wave based methods are still challenging. Requirement of trained and experienced operator, limited application area, need of coupling between two-surfaces in case of contact based technique are common constraints in the application of guided-wave based methods. Additionally, a long inspection time also hampers operation of the system. Recent research on air-coupled or non-contact coupling methods, development of fully automated system has relaxed the obscurity to some extent. Most of the ultrasonic based methods are efficient in determining material degradation or micro-crack in a plate or thin-walled structures. On the contrary, vibration based methods are less sensitive to micro-crack and complicated in solving theoretical or numerical evaluation of nonlinear breathing crack. The present study hence aimed at attracting researchers’ attention in the advancement of existing techniques to detect breathing crack or micro-crack with improved sensitivity and versatility.

Many reviews have been performed in the past on nonlinear system identification methods, analysis of vibration characteristics of different members [5], application of nonlinear dynamics on SHM [39], modeling of nonlinear crack-wave interaction [40], etc.

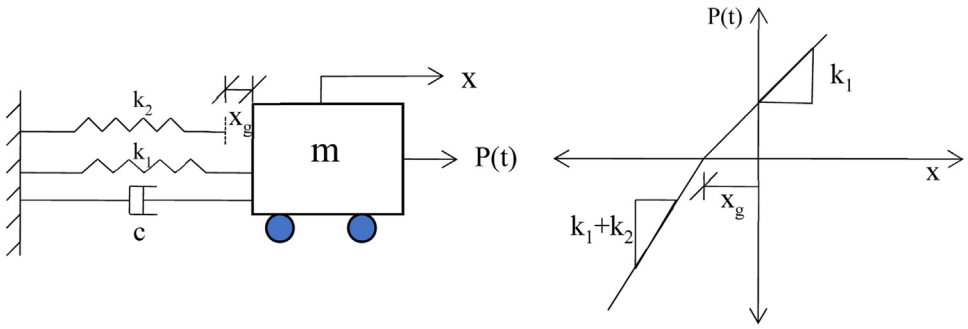


**Fig. 1.** (a) Schematic representation of breathing crack with SDOF spring-mass system, and (b) force-displacement diagram.

However, to the best of author's knowledge a complete review dedicated to the nonlinear breathing crack from modeling to different damage detection techniques is not taken up before.

The present review summarizes a number of techniques associated with the solution and identification of breathing crack to expand their implementations. The study also upholds the potential and limitations of different methods to light up the required areas of improvement in future. With this aim, the whole review is organized as follows. At first, the behavior of a breathing crack is mathematically explained to give an insight into the embedded nonlinear characteristics. Some system identification techniques and methods of solution of nonlinear equations applied for breathing crack identification are then reviewed. Limitations and advantages of different nonlinear methods are highlighted therein. Since, nonlinear dynamics is a vast topic of research, an exhaustive list of methods could not be reviewed in a single article. A few state-of-the-art methodologies are selected in this work to reflect an overview about the difficulties and prospect in identification of nonlinear behavior of cracks for the early prediction of damage. Next, an overview of different modeling approaches; theoretical, numerical, and experimental modeling of breathing crack is discussed. Finally, the future scope of nonlinear analysis for the detection of very small damage in structure is presented in the conclusion section.

*Insight to breathing mechanism with equation of motion*

In Fig. 1, the mechanism of breathing crack is shown with a single DoF system. The change in stiffness of this system depends on the position of mass $m$ which is again a function of time $t$. When stiffness of both spring $k_1$ *and* $k_2$ contributes to the total stiffness $k$ of the system, it restores the undamaged state. Otherwise, it represents a damaged state. Here, the excitation force $P(t)$ is shown to have applied along positive $x$ direction. Under the action of force when position of mass is $x \leq x_g$, total stiffness of the system becomes summation of $k_1$, $k_2$ and for $x \geq x_g$ only stiffness $k_1$ contributes to the total stiffness of the system. This variation of stiffness is explained graphically through the force-displacement diagram in Fig. 1(b). The equation of motion of the system is shown in Eqs. (1) and (2) defines the stiffness variation as a function of displacement. It can be seen from this equation that depending on the position of mass, the system will have two different stiffness

$$m\ddot{x} + c\dot{x} + k(x)x = P(t); \tag{1}$$

$$k(x) = \begin{cases} k_1 + k_2 \; ; x \leq x_g \\ k_1 ; x > x_g \end{cases} \tag{2}$$

values. It thus results in two natural frequencies $\omega_1$ and $\omega_2$. It is reported by Yan et al. [32] that in the case of free-vibration of the system, frequency of the whole system $\omega_0$ is related to these two frequencies by Eq. (3).

$$\omega_0 = \frac{2\,\omega_1\,\omega_2}{\omega_1 + \omega_2} \tag{3}$$

If the period for $\omega_1 = 2\pi/T_1$ and $\omega_2 = 2\pi/T_2$, then total period $T$ of the system will be $(T_1/2 + T_2/2)$. From free-vibration responses, it has been observed that for systems with bilinear stiffness total period does not vary which may not be the case for other nonlinear systems. Different theory for stiffness variation in presence of breathing crack is proposed by various researchers in the past. It is discussed in the subsection 'Analytical modeling' under the section 'Modeling of breathing crack'. The nonlinear features though sensitive to damage may get suppressed by similar features developed by various sources of noise. These noises present similar characteristics in the frequency spectrum as a nonlinear response. It is thus difficult to isolate the original behavior of the structure from measured responses. The above two challenges; (a) solution of nonlinear equations and (b) identification of the presence of nonlinearity and its source have been addressed in many recent studies [41–43]. However, a global method applicable to every type of nonlinear problem is still unknown. Gudmundson [42] compared the effect of breathing crack on the natural frequency of the system. The analysis is performed on a cantilever beam with a sine-sweep signal generator. Perturbation method is used to solve the finite element equations. Different crack locations and crack lengths are chosen to observe the effect on the first few eigenfrequencies. For small crack, frequencies of beam computed considering breathing crack almost matched with open crack model. With the increase in crack length, residual stress is developed at the crack tip. This residual stress acts against the opening of the crack and during vibration it results in partial closure of the crack. Hence, the natural frequency of the member with a breathing crack falls between frequency

of the member with a fully open crack and the state when crack is completely closed. Behavior and impact of breathing crack on the dynamic response are further investigated by several researchers to develop new methods for the detection and localization of early cracks in the member. Most studies have established a relationship between harmonics obtained from the frequency response with the existence of breathing cracks. The amplitude of these harmonics depends on many factors including modeling technique and solution procedure. Among these, some of the promising methods are reviewed in the present article.

## Identification of breathing crack by vibration based methods

### *Expansion series based methods and correlation with Volterra series*

The development of nonlinear dynamics in the last few years has decoded various unique features embedded in the response. The time-variant stiffness characteristics of a system with breathing crack made it possible to apply the nonlinear system identification technique for ensuring presence of the smallest crack in the structure. There are various expansion series available to model a nonlinear system such as Volterra series, Wiener series, Taylor series, etc. However, all series are closely connected to Volterra series as described by Cheng et al. [49]. Hence, this section first describes the development of the Volterra series as an efficient solution method for nonlinear systems in the time domain. Then, different methods evolved for the simplified application of Volterra functions are discussed concerning the identification of breathing cracks. The Volterra series has been established as the foundation of several advanced methods developed for the identification of nonlinearity. Practically, the behavior of a structure may not completely follow linear assumptions made for the assessment of response. This is because of the formation of additional resonating frequency components of the system. In presence of nonlinearity, a part of the energy transfers to the higher harmonic components. It results in the generation of additional frequency components other than natural frequency and forcing frequency of the system. To define this type of system, Volterra series is developed by extending convolution integral form of linear system to nonlinear one. If a linear system is excited by a unit impulse Dirac function at $\tau$ secs earlier, the response of the signal $x(t)$ at time $t$ is defined by Eq. (4).

$$x(t) = \sum h(\tau)\delta(t-\tau)\Delta\tau; \tag{4}$$

Here, $h(\tau)$ is the response at unit impulse. If an impulse force of amplitude $p$ is applied for a short time duration, the response of the linear system is expressed as Eq. (5).

$$x(t) = \sum h(\tau)p\delta(t-\tau)\Delta\tau \tag{5}$$

The input signal with amplitude $p$ applied for a short time duration can also be represented as (Eq. (6)),

$$p(t-\tau)\Delta\tau = p\delta(t-\tau)\Delta\tau, \ \& \ P(t) = \sum p\delta(t-\tau)\Delta\tau \tag{6}$$

Replacing the Dirac function in Eq. (4) by the input forcing function, the total response $x(t)$ for a series of impulse input signals can be written as,

$$x(t) = \sum h(\tau)p(t-\tau)\Delta\tau \tag{7}$$

When $d\tau \to 0$, the approximated input signal in Eq. (7) transforms to a more accurate representation of the excitation signal. The output response is then written as,

$$x(t) = \int_0^\infty h(\tau)p(t-\tau)d\tau \tag{8}$$

The expression of output signal in Eq. (8) for any type of excitation is only possible where the principle of superposition is applicable and the scaling of output remains same as the input signal. This is the main constraint for the application of the above convolution integral technique in nonlinear systems. In Eq. (1), the variation of stiffness can be represented in a polynomial form by Eq. (9).

$$m\ddot{x} + c\dot{x} + kx(t) + \sum_{i=2}^{n} k_i x^i(t) = P(t); \ i \text{ is an integer} \tag{9}$$

$k_i$ is the nonlinear stiffness. The above nonlinear system can behave linearly when the value of $x^i(t)$ is so small that its multiplication with nonlinear stiffness parameter $k_i x^i(t) \to 0$ for $i \geq 2$. The physical significance of this first condition is that a nonlinear system behaves linearly when the external forcing amplitude is very small. Also, in case of nonlinear stiffness parameter $k_i = 0$ and the same equation defines a linear system. Now, if the Eq. (9) is used for the evaluation of a nonlinear system response under Dirac forcing function, an error $o(\varepsilon_1)$ will occur. The magnitude of $o(\varepsilon_1)$ (Eq. (10)) depends on the system parameter and amplitude of the excitation force.

$$x(t) = \sum h_1(\tau_1)\delta(t-\tau_1)\Delta\tau_1 + o(\varepsilon_1) \tag{10}$$

Similarly for two impulses with time delay $\Delta\tau_1$ and $\Delta\tau_2$

$$x(t) = \sum h_1(\tau_1)\delta(t-\tau_1)\Delta\tau_1 + \sum h_1(\tau_2)\delta(t-\tau_2)\Delta\tau_2 + o(\varepsilon_2) \tag{11}$$

The error value $o(\varepsilon_2)$ in Eq. (11) is more than $o(\varepsilon_1)$ as the impulse force continues to be summed up to represent the original input signal. The appearance of nonlinearity can be defined as the interaction between responses under each impulse. Hence, incorporating

an extra term as a function of product of two response amplitude, the value of $o(\varepsilon_2)$ can be minimized. The above response thus can be modified more accurately as,

$$x(t) = \sum h_1(\tau_1)\delta(t-\tau_1)\Delta\tau_1 + \sum h_1(\tau_2)\delta(t-\tau_2)\Delta\tau_2 + \sum\sum h_2(\tau_1,\tau_2)\delta(t-\tau_1)\delta(t-\tau_2)\Delta\tau_1\Delta\tau_2 + o(\varepsilon_{21}) \tag{12}$$

Here in Eq. (12),

$$o(\varepsilon_2) = \sum_{\tau_1<t}\sum_{\tau_2<t} h_2(\tau_1,\tau_2)\delta(t-\tau_1)\delta(t-\tau_2)\Delta\tau_1\Delta\tau_2 + o(\varepsilon_{21}) \tag{13}$$

The additional term in Eq. (13). is called second-order impulse response function. For a continuous input signal, if $n$ number of impulses are considered to approximate the excitation input and if $\tau_i = n\Delta\tau_i$, the generalized response at any time instant $t$ can be written as,

$$\begin{aligned} x(t) = &\sum_{i=1}^{n} h_i(\tau_i)\delta(t-\tau_i)\Delta\tau_i + \sum_{i_1=1}^{n}\sum_{i_2=1}^{n} h_2\left(\tau_{i_1},\tau_{i_2}\right)\delta\left(t-\tau_{i_1}\right)\delta\left(t-\tau_{i_2}\right)\Delta\tau_{i_1}\Delta\tau_{i_2} + \dots \\ &+ \sum_{i_1=1}^{n}\dots\dots\sum_{i_n=1}^{n} h_n(\tau_{i_1},\tau_{i_2},\dots..\tau_{i_n})\delta\left(t-\tau_{i_1}\right)\,\delta\left(t-\tau_{i_1}\right)\dots\dots\delta\left(t-\tau_{i_n}\right)\Delta\tau_{i_1}\Delta\tau_{i_2}\dots.\Delta\tau_{i_n} + o(\varepsilon_n) \end{aligned} \tag{14}$$

The value of $o(\varepsilon_n)$ in depends on the degree of higher-order response function. Response of a system subjected to idealized discrete input is given by Eq. (14). If the signal is continuous over time, i.e. if $\Delta\tau_i \to 0$, $n \to \infty$ and arbitrary input $P(t) = \int_0^\infty p(t-\tau)d\tau$, the infinite series of output signals is represented as,

$$\begin{aligned} x(t) = &\int_0^\infty h_i(\tau_i)p(t-\tau_i)d\tau + \int_0^\infty\int_0^\infty h_2(\tau_1,\tau_2)p(t-\tau_1)p(t-\tau_2)d\tau_1 d\tau_2 + \dots \\ &+ \int_0^\infty\dots\dots\int_0^\infty h_n(\tau_1,\tau_2,\dots\tau_n)p(t-\tau_1)\;p(t-\tau_1)\dots p(t-\tau_n)d\tau_1 d\tau_2\dots d\tau_n \end{aligned} \tag{15}$$

For a casual system, the response of which does not depend on the input function of future, as assumed for a Volterra series, the limit of Eq. (15) can be extended to $-\infty$ *to* $+\infty$ from 0 to $+\infty$. The casualty of the series also stipulates that if any of the arguments $\tau_1, \tau_2, \dots, \tau_n$ is negative, the Volterra kernel $h_n(\tau_1, \tau_2, \dots \tau_n)$ will be zero. Hence,

$$\begin{aligned} x(t) = &\int_{-\infty}^\infty h_i(\tau_i)p(t-\tau_i)d\tau + \int_{-\infty}^\infty\int_{-\infty}^\infty h_2(\tau_1,\tau_2)p(t-\tau_1)p(t-\tau_2)d\tau_1 d\tau_2 + \dots \\ &+ \int_{-\infty}^\infty\dots\dots\int_{-\infty}^\infty h_n(\tau_1,\tau_2,\dots\tau_n)p(t-\tau_1)\;p(t-\tau_1)\dots p(t-\tau_n)d\tau_1 d\tau_2\dots d\tau_n \\ = &\, x_1(t) + x_2(t) + \dots + x_n(t) = \sum_{n=1}^{N} x_n(t) \end{aligned} \tag{16}$$

$N$ in Eq. (16) is the highest-order of nonlinearity considered for the close approximation of nonlinear output by Volterra series. The total response is thus represented as the combination of responses from each individual component. The $n^{th}$-order response component is given in Eq. (17).

$$x_n(t) = \int_{-\infty}^\infty\dots\dots\int_{-\infty}^\infty h_n(\tau_1,\tau_2,\dots\tau_n)p(t-\tau_1)\;p(t-\tau_1)\dots p(t-\tau_n)d\tau_1 d\tau_2\dots d\tau_n \tag{17}$$

For a harmonic input force $Pe^{j\omega t}$ the higher order response becomes,

$$x_n(t) = (Pe^{j\omega t})^n\int_{-\infty}^\infty\dots\dots\int_{-\infty}^\infty h_n(\tau_1,\tau_2,\dots\tau_n)\prod_{i=1}^{n} e^{-j\omega_i\tau_i}d\tau_i = (Pe^{j\omega t})^n H_n(\omega_1,\omega_2,\dots,\omega_n) \tag{18}$$

The Volterra series is defined by Eq. (18) and higher-order impulse response functions in this equation are called kernels of this series. The kernel function characterizes the behavior of the system. Hence, identification of any system using Volterra series requires the determination of kernels from the measured data. The form of the equation entails that it is applicable for those nonlinear systems where system parameters remain constant over time. However, in many structural systems, system parameters are variable. It imposes a restriction on the successful application of Volterra series in the parametric characterization of all types of nonlinear systems. Eq. (18) can also be written in the frequency domain using definition of higher-order FRF for single harmonic input with frequency $\omega$ by Eq. (19).

$$\begin{aligned} &x_n(t) = (Pe^{j\omega t})^n H_n(\omega,\omega,\dots,\omega) \\ &\text{Therefore,} \qquad x(t) = H_1(\omega)(Pe^{j\omega t}) + H_2(\omega,\omega)(Pe^{j\omega t})^2 + \dots + H_n(\omega,\omega,\dots,\omega)(Pe^{j\omega t})^n \end{aligned} \tag{19}$$

If a sinusoidal wave is defined as $Pcos(\omega t) = \frac{P}{2}e^{j\omega t} + \frac{P}{2}e^{-j\omega t}$, output response can be defined in the form of Volterra series by Eq. (20).

$$\begin{aligned} x(t) = &H_1(\omega)\left(\frac{P}{2}e^{j\omega t}\right) + H_1(-\omega)\left(\frac{P}{2}e^{-j\omega t}\right) + H_2(\omega,\omega)\left(\frac{P}{2}e^{j\omega t}\right)^2 + H_2(-\omega,-\omega)\left(\frac{P}{2}e^{-j\omega t}\right)^2 + H_2(-\omega,\omega)\left(\frac{P}{2}\right)^2 \\ &+ H_2(\omega,-\omega)\left(\frac{P}{2}\right)^2 + \dots + n^{th}\ terms \end{aligned} \tag{20}$$

Here the expression is terminated at $n^{th}$-order FRF. Now, considering homogeneity of Volterra series, the above equation is simplified as,

$$\begin{aligned} x(t) &= H_1(\omega)\left(\frac{P}{2}e^{j\omega t}\right) + H_1(-\omega)\left(\frac{P}{2}e^{-j\omega t}\right) + H_2(\omega,\omega)\left(\frac{P}{2}e^{j\omega t}\right)^2 + H_2(-\omega,-\omega)\left(\frac{P}{2}e^{-j\omega t}\right)^2 \\ &\quad + 2H_2(-\omega,\omega)\left(\frac{P}{2}\right)^2 + \ldots + n^{th}\ terms \\ &= 2\left|H_1(\omega)\right|\left(\frac{P}{2}\right)\cos\left\{\omega t + \angle H_1(\omega)\right\} + 2\left|H_2(\omega,\omega)\right|\left(\frac{P}{2}\right)^2\cos\left\{2\omega t + \angle H_2(\omega,\omega)\right\} \\ &\quad + 2H_2(-\omega,\omega)\left(\frac{P}{2}\right)^2 + \ldots n^{th}\ terms \end{aligned} \tag{21}$$

It is evident from Eq. (21), that for a nonlinear system subjected to single harmonic force as input, the output response will be comprised of several harmonic signals of integer multiple of forcing frequencies along with a shift in phase. Hence, the presence of harmonics in the frequency response spectrum is considered as one of the nonlinear system identification techniques. However, it is difficult to extract frequency response function (FRF) of each frequency component from the total response data. The difficulties in directly obtaining Volterra kernel functions have also been addressed in many researches for the identification of breathing cracks in a structure. Fourier transformation, correlation measurement, polyspectral analysis, etc. are some of the methods developed based on Volterra series. Lin and Ng [44] proposed a new method using correlation techniques for the measurement of higher-order frequency response function (HOFRF). The use of this correlation technique is easy to implement and eliminates some of the drawbacks of Fourier transformation which occur due to leakage, aliasing effect, etc. In this process, the measured output signal is multiplied by the $e^{jn\omega t}$; where $n\omega$ is the intended higher-order frequency and integrated over a long period of time after the decay of transient motion. The response corresponding to that harmonic frequency is then subtracted from the total response and again followed the same step for another higher-order response function $H_n(\omega,\omega,\ldots,\omega)$, where $n$ is the order of FRF. However, this method is suitable when the input signal is purely sinusoidal wave. In practical scenario, an input sinusoidal wave may get distorted due to various sources of noise which may in turn affect the supremacy of the method. Peng et al. [22] demonstrated the application of new NOFRF based concept developed from Volterra series as an indicator of breathing crack. Lang and Billings [45] extended the relationship of input and output frequency spectrum of a linear system to nonlinear one by applying Volterra series. If input excitation in frequency domain is $P(\omega)$ and corresponding output frequency spectra is denoted as $X(\omega)$, for a linear system the relationship is expressed as Eq. (22). In this equation, $H(\omega)$ is FRF of the linear system.

$$X(\omega) = H(\omega)\ P(\omega \tag{22}$$

Similarly, performing Fourier transform on Volterra series the relationship can be established as,

$$X(j\omega) = \sum_{n=1}^{N} X_n(j\omega); \tag{23}$$

$$X_n(j\omega) = \frac{1/\sqrt{n}}{(2\pi)^{n-1}}\int_{(\omega_1+\omega_2+\ldots+\omega_n=\omega)} H_n(j\omega_1, j\omega_2, \ldots, j\omega_n)\prod_{i=1}^{n} P\left(j\omega_i\right)d\vartheta_{n\omega} \tag{24}$$

The above Eqs. (23) and (24) can also be re-written as

$$X_n(j\omega) = \frac{\int_{(\omega_1+\omega_2+\ldots+\omega_n=\omega)} H_n(j\omega_1, j\omega_2, \ldots, j\omega_n)\prod_{i=1}^{n} P\left(j\omega_i\right)d\vartheta_{n\omega}}{\int_{(\omega_1+\omega_2+\ldots+\omega_{n=\omega})}\prod_{i=1}^{n} P\left(j\omega_i\right)d\vartheta_{n\omega}} \times \frac{1/\sqrt{n}}{(2\pi)^{n-1}}\int_{(\omega_1+\omega_2+\ldots+\omega_n=\omega)}\prod_{i=1}^{n} P\left(j\omega_i\right)d\vartheta_{n\omega}$$

This is valid when $\int_{(\omega_1+\omega_2+\ldots+\omega_n=\omega)}\prod_{i=1}^{n} P(j\omega_i)d\vartheta_{n\omega} \neq 0$;

$$= G_n(j\omega)\ P_n(j\omega) \tag{25}$$

Here,

$$G_n(j\omega) = \frac{\int_{(\omega_1+\omega_2+\ldots+\omega_n=\omega)} H_n(j\omega_1, j\omega_2, \ldots, j\omega_n)\prod_{i=1}^{n} P\left(j\omega_i\right)d\vartheta_{n\omega}}{\int_{(\omega_1+\omega_2+\ldots+\omega_n=\omega)}\prod_{i=1}^{n} P\left(j\omega_i\right)d\vartheta_{n\omega}}\ P_n(j\omega) = \frac{1/\sqrt{n}}{(2\pi)^{n-1}}\int_{(\omega_1+\omega_2+\ldots+\omega_n=\omega)}\prod_{i=1}^{n} P\left(j\omega_i\right)d\vartheta_{n\omega} \tag{26}$$

Replacing the value of Eq. (25) in Eq. (23) we get,

$$X(j\omega) = \sum_{n=1}^{N} G_n(j\omega)\ P_n(j\omega) \tag{27}$$

The expression is analogous to linear system. The term $G_n(j\omega)$ in Eq. (26) allows the output frequency response function of a nonlinear system to be expressed in the similar way as linear system. $G_n(j\omega)$ is called NOFRF. From the expression of $G_n(j\omega)$ it can be proved that this NOFRF is insensitive to any linear gain in input spectrum. The peak in the spectrum of $G_n(j\omega)$ indicates that the contribution of input to $n^{th}$ order output is enhanced at this frequency. If the frequency peak $G_n(j\omega)$ lies outside the input frequency band, generation of outside band components is considered to be due to the effect of nonlinearity of the system. This characteristic is

applied by Peng. et al. [22] for the detection of breathing-crack nonlinearity. In case of $P(t) = \alpha\bar{P}(t)$, where α is a constant and $\bar{P}(t)$ is the input signal required to excite the structure for the evaluation of NOFRF,

$$P_n(j\omega) = \alpha^n \frac{1/\sqrt{n}}{(2\pi)^{n-1}} \int_{(\omega_1+\omega_2+\ldots+\omega_n=\omega)} \prod_{i=1}^{n} \bar{P}(j\omega_i)\, d\vartheta_{n\omega};\ \text{and}$$

$$P_n(j\omega) = \alpha^n \bar{P}_n(j\omega)$$

$$X(j\omega) = \sum_{n=1}^{N} \alpha^n \bar{G}_n(j\omega)\ \bar{P}_n(j\omega) \tag{28}$$

$d\vartheta_{n\omega}$ denotes a small element in the integral field or hyperplane which satisfies the constraint $(\omega_1 + \omega_2 + \ldots + \omega_n = \omega)$. In matrix form, Eq. (28) can be represented by Eq. (29).

$$[X(j\omega)] = \left[\alpha\bar{P}_1(j\omega),\ \alpha^2\bar{P}_2(j\omega), \ldots, \alpha^n\bar{P}_n(j\omega)\right]\left[\bar{G}_n(j\omega)\right] \tag{29}$$

To solve the system of equations, the structure needs to be excited $\bar{N}$ times with different input signals $P_i(t) = \alpha_i\bar{P}_i(t)$; where $= 1, 2, \ldots,\ \bar{N}$ . The value of $\bar{N}$ should be selected in such a way that it is greater than the highest-order of frequency response function $N$ considered in Volterra series to define the output spectrum of the nonlinear system. The value of constant $\alpha$ should be incremental such as $\alpha_i < \alpha_{i+1}$. The NOFRF spectrum in the form of $[\bar{G}_n(j\omega)]$ is then evaluated as given in Eq. (30).

$$\begin{aligned} &[X(j\omega)] = A\bar{P}_{1,2,\ldots,\bar{N}}(j\omega)\ \left[\bar{G}_n(j\omega)\right] \\ &\text{Therefore,} \qquad \left[\bar{G}_n(j\omega)\right] = \left[\left(A\bar{P}_{1,2,\ldots,\bar{N}}(j\omega)\right)^T\left(A\bar{P}_{1,2,\ldots,\bar{N}}(j\omega)\right)\right]^{-1}\left(A\bar{P}_{1,2,\ldots,\bar{N}}(j\omega)\right)^T[X(j\omega)] \end{aligned} \tag{30}$$

The NOFRF spectrum analysis under different excitations [22] has shown that the amplitude of harmonics depends on the excitation amplitude as well as degree of nonlinearity or size of crack depth. For small crack size, the amplitude of harmonics is found to be difficult to distinguish from the spectrum of undamaged state. A similar condition is observed for weak excitation. In case of weak excitation, the crack may not be closed during vibration and thus appears with low amplitude harmonics difficult to isolate. With the increase of excitation amplitude, the crack completely gets closed and enhances the frequency amplitude of harmonics other than primary resonance frequency. A strong excitation may also result in the geometric nonlinearity effect along with the contact nonlinearity of breathing crack. This may reduce the efficiency of the detection of breathing cracks. The advantage of NOFRF is that it is a one-dimensional function in contrast to general frequency response function (GFRF) which is multi-dimensional in nature. It eases the solution procedure of the determination of NOFRF and thus the behavior of structural system in presence of crack. Cheng et al. [46] utilized the potential of NOFRF in locating damage by identifying local nonlinearity in a 2D-periodic member. It is evident from the expression of GFRF and NOFRF expression that both of these forms of nonlinear system analysis can not be related directly to the nonlinear characteristics parameters and output spectrum of the system. This problem is addressed in the work of Peng et al. [22]. Output frequency response function (OFRF) is proposed by directly linking nonlinear parameters with the output spectrum in frequency domain. The governing nonlinear differential equation is expressed in the polynomial form of system parameters. It thus facilitates in understanding the impact of system parameters on the output frequency response explicitly which is an advantage over previously developed methods GFRF and NOFRF. Another frequency response function is developed by Feijoo et al. [47] to overcome the problem of multi-dimensionality of GFRF method. The function is termed as Associated frequency response function (AFRF) which uses combination function of lower-order Volterra output as the input of an associated linear system (Eq. (31)). It is expressed as Eq. (31).

$$Lx_n = f\left(x_1, x_2, \ldots.\ x_{n-1}\right) \tag{31}$$

Where $L$ is a linear operator of nonlinear differential equation and $x_n(t)$ is defined as Eq. (32).

$$x_n(t) = \int_{-\infty}^{\infty} \ldots \int_{-\infty}^{\infty} h_n(\tau_1, \tau_2, \ldots, \tau_n) \prod_{i=1}^{n} [x(t-\tau_i)\, d\tau_i] \tag{32}$$

The whole algorithm of AFRF analysis can be represented through a flowchart (Fig. 2) which solves $x(t)$ as a combination of $n^{th}$ order of associated linear equations (ALE).

In the above discussion, various models are described which have been established in the past for the classical solution of nonlinear systems. In such cases, it is required to know the mathematical description of the model a-priori in which nonlinear parameters are expressed in a polynomial form. The analytical modeling of breathing crack proposed by different researchers is described in detail in the 'Theoretical modeling of breathing crack' section. It shows that even the breathing crack phenomenon can be defined in the form of polynomials where stiffness is considered as a time-variant function. Owing to this, the characteristics of breathing crack resemble the behavior of a nonlinear system and validate the application of above models to serve different levels of SHM. As Volterra series expansion contains infinite number of terms, it necessitates the series to be tested for convergency to get an appropriate solution when higher harmonics with dominant effects are present. This drawback limits its use in strong-nonlinear systems.

*Coherence based methods for identification of breathing cracks*

The analysis of structural behavior from a polluted measured signal is always a difficult task. Among different other nonlinear system identification techniques, coherence-based analysis is found to have significant attention in the development of damage

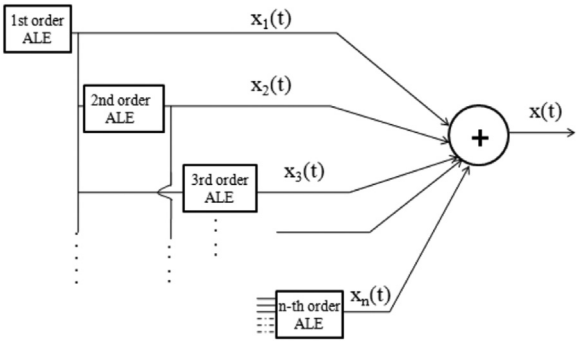


**Fig. 2.** Flow-chart of AFRF analysis procedure.

indicators for breathing cracks. A brief review is furnished to elaborate the application of higher-order coherence analysis in the identification of breathing crack. It showed promising results in the past over other higher order statistical methods. Higher order coherence-based analysis shows promising results if a structure is vibrated within an intended frequency band. The higher-order moment of time-series signal which is also called higher-order coherence can be used for the detection and localization of breathing cracks. Among various higher-order statistical-based analyses, bicoherence is the most common and simplest method employed by many researchers to check nonlinearity in the signal [48,49]. Choudhury et al. [50] proposed nonlinearity index to quantitatively compute the degree of nonlinearity in the signal. The index is based on the bicoherence value of the signal. Bicoherence is a normalized form of bi-spectrum. It is estimated in following steps:

(a) At first, sampling frequency $f_s$ of the measured time series is checked against Nyquist frequency $f_{Nq}=1/2\Delta t$. $\Delta t$ is the time interval. The sampling frequency should be much smaller than $f_N$.
(b) The number of dataset records is $n$. Total number of data points in each record is 2 N. Then record time $T = 2N\Delta t$. The measured time series at any time $t$ is then expressed as $x^{(i)}(k)$; where $i$ = 1,2…n and $k$ = 1,….2 N. Here $x(k)$ means value of $x$ at time $t = k\Delta t$. Find out the mean value of each of the $n$ records. This mean value is subtracted from each of the corresponding time series.
(c) An appropriate window frame for each recorded data is choosen.
(d) Time-series of each segment is transformed by DFT or FFT to frequency domain with frequency amplitude $X(f_k)$.
(e) Bi-spectrum of the time signal is then computed with the following Eq. (33) [51].

$$bis(f_l, f_m) = \frac{\sum_{i=1}^{n} X_i(f_l) * X_i(f_m) * \overline{X_i}(f_l+f_m)}{n} \tag{33}$$

$\overline{X_i}(f_l + f_m)$ is complex conjugate.

(f) Bicoherence of the signal is then calculated by normalizing the value of bispectrum in the following way (Eq. (34)).

$$bic^2 = b^2(l,m) = \frac{\left|bis(f_l, f_m)\right|^2}{\left(\frac{\sum_{i=1}^{n} |X_i(f_l) * X_i(f_m)|^2}{n}\right)\left(\frac{\sum_{i=1}^{n} |X_i(f_l+f_m)|^2}{n}\right)} \tag{34}$$

In order to avoid ill-conditioned singularities due to low value at the denominator, a factor $\epsilon$ is added.

$$bic^2 = b^2(l,m) = \frac{\left|bis(f_l, f_m)\right|^2}{\left(\frac{\sum_{i=1}^{n} |X_i(f_l) * X_i(f_m)|^2}{n}\right)\left(\frac{\sum_{i=1}^{n} |X_i(f_l+f_m)|^2}{n}\right) + \epsilon} \tag{35}$$

(g) Nonlinear index (NLI) $= b^2(l,m)_{max} - \left(b^2(l,m)_{mean} + 2\sigma^*_{bic^2} b^2(l,m)\right)$ (36)

In Eq. (35), $b^2(l,m)$ is the bicoherence function that estimates the interaction between two frequencies $f_l$ and $f_m$ in generating coupled frequency as the summation of $f_l$ and $f_m$. The nonlinear index derived from the bicoherence equation is depicted in Eq. (36). $\sigma^*$ is the standard deviation of bicoherence. Zero bicoherence value indicates $f_l + f_m$ is an independent frequency developed without any interaction between two frequencies $f_l$ and $f_m$. If the value is 1, it signifies the formation of $f_l + f_m$ by the full interaction between $f_l$, and $f_m$. In this way, the presence of nonlinearity in the signal is assured. Sometimes the denominator of the bicoherence function may become too small and result in the generation of false peaks in the coherence spectra. To minimize this effect, an additional factor $\epsilon$ is used in the denominator with a suitable value to suppress the spurious peaks in the frequency spectrum. The harmonics are generated in the multiple of the primary resonance frequency. Hence bicoherence is measured between three harmonic frequency components. For example, $b^2(1,2)$ measures bicoherence of 1x, 2x and (1 + 2)=3x multiple of harmonics. Thus, if harmonics

are generated by the coupling of two frequencies it will have a closer value to 1 indicating a nonlinear response. This capacity of bicoherence function in isolating system-generated nonlinearity from noise is applied to detect and localize the presence of crack. For the damage localization, the length of the member is divided by distributed nodes, and total nonlinearity index (TNLI) [49] value is computed at each node. Nodes with the highest values of NLI are considered as the probable position of damage with breathing behavior.

Similarly, tri-coherence can also be computed as another higher-order coherence analysis as proposed by Sinha [52]. In this analysis, interaction of four frequencies is investigated. The tri-coherence function is represented as $Tri_{\mathrm{lmq}}$. Here, $Tri$ denotes tri-coherence function $l, m, q$ in the subscript are three independent frequencies to be analyzed to check possible interaction in the occurrence of frequency $l + m + q$ by their coupling. Different types of vibration data from periodic to random have been investigated for the analysis of bicoherence performance. In each case, it has shown great potential for practical application. The coherence analysis is superior in terms of simplicity among other higher-order statistical tools. It can measure nonlinearity directly from the measured data which is an advantage in the real field application. However, the averaging process requires a large number of long time data records to reflect structural behavior with great accuracy.

*Numerical methods for breathing crack induced nonlinear system identification*

The formulation of classical models includes a large number of higher-order terms for the actual description of output response. It incorporates a truncated error in the approximated value of output response determined by the above models. The magnitude of truncated error grows with the degree of nonlinearity. For a strong nonlinear system, no methods are yet developed to characterize the unpredictable behavior of the nonlinear system. Some numerical methods are developed in an attempt to explain the behavior of such nonlinear systems which are discussed in the next section. Ruotolo et al. [19] analyzed a cantilever beam by harmonic balance method (HBM). To apply this method the closing crack function is expressed in the form of Fourier series as given in Eq. (37). In HBM analysis, the solution of nonlinear equation is considered to be the summation of several harmonics with frequencies integer multiple of forcing frequency. Thus, the solution of equation of motion in a truncated Fourier series form is assumed as (Eq. (37)),

$$x(t) = a_0 + \sum_{n=1}^{\bar{n}} a_n \sin(n\omega t) + b_n \cos(n\omega t) \tag{37}$$

Here $\bar{n}$ is the number of harmonics to be considered for the evaluation of response. $a_0$, $a_i$ and $b_i$ are Fourier coefficients of $n^{th}$ harmonic (Eq. (38)).

$$a_0 = \frac{1}{T}\int_t^{t+T} x(t)dt,\ a_n = \frac{2}{T}\int_t^{t+T} x(t)\cos\ (i\omega t)dt,\ \text{and}\ b_n = \frac{2}{T}\int_t^{t+T} x(t)\sin(i\omega t)dt \tag{38}$$

The use of HBM method is the simplest and easier than other numerical methods. When nonlinearity of a system is weak in nature, higher harmonics will have little impact on the system's response. However, in case of strong nonlinearity higher harmonics become dominant, and response under these harmonics needs to be determined in order to correctly represent the output response. In such cases, truncated Fourier series expression fails to identify actual response of the system. Numerical analysis is also cumbersome to perform as the expression under higher-order harmonics becomes complex. It is evident in the work of Peng et al. [53] where a comparison is made between the efficiency of Volterra series expansion and harmonic balance method. The analysis performed on a duffing oscillator reveals different features of these two methods. HBM method is advantageous in describing jump phenomenon captured at a certain frequency range of vibration if the system is nonlinear. It takes a quite long time to solve the set of nonlinear equations when higher-order harmonics are involved. The formation of super and subharmonic resonance in the spectra can't be theoretically explained by this analysis. On the other hand, Volterra series-based nonlinear frequency response function has a robust classical background in describing the appearance of harmonics by the energy transfer mechanism under nonlinear vibration. The requirement of computational time is not a constraint for this method. However, the definition of NOFRF or underlying Volterra series does not exist at any discontinuous point referring to the incapability in capturing jump phenomenon, unlike HBM. Another numerical method, perturbation technique is developed [54] to solve weakly nonlinear systems. The study shows that approximate solution by Regular Perturbation (RP) method may include secular terms in the solution. The solution thus becomes divergent when it is sought for a long time. To mitigate this problem, numerous improved methods have been developed such as homotopy-perturbation method [55], multiple-time scale method [56], lindstedt-Poincaré (L-P) method [57], etc. Dong et al. [58] numerically analyzed a polynomial nonlinear system and found differences in the result obtained from the perturbation method and Volterra series expansion. It reveals that for a damped dissipative system perturbation method and Volterra series-based steady-state response completely coincide with each other. Runge-Kutta-based method on the other hand produced almost identical results except a fourth harmonic of small amplitude additionally appeared in the frequency spectra, unlike the other two methods. The truncation of the perturbation method and Volterra series in third order is the reason behind not showing up the fourth-harmonic in the steady-state response spectra. A response analysis is also performed on undamped conservative system. The Fourier transformation result of the response computed by Runge-Kutta method, Volterra series, and perturbation method is presented in Fig. 3 for both damped and undamped systems. It clearly shows a visible difference in the frequency spectra. Runge-Kutta method and RP method-based frequency spectra produce a similar type of spectrum after Fourier transformation of steady-state response. On the contrary, the peak value of harmonics estimated from Volterra series though close to the other two methods, frequency spectrum is not completely identical.

Long et al. [59] applied multi-scale method for the vibration analysis of a cracked beam. Several super-harmonic and sub-harmonic frequencies in the spectrum that indicates system nonlinearity, are successfully produced by Fourier transformation of the results

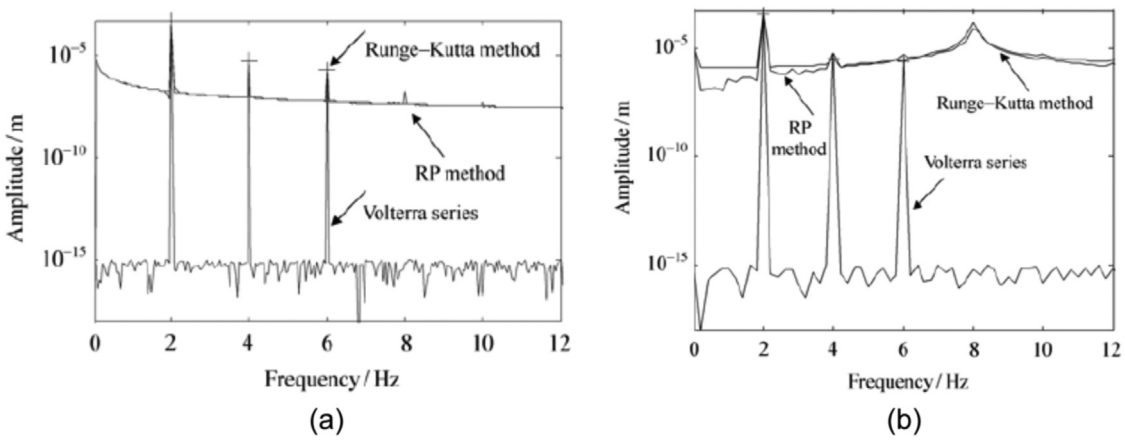


**Fig. 3.** Fourier transformation of steady-state response estimated by RP method, Volterra series, and Runge-Kutta method for (a) damped dissipative system, and (b) undamped conservative system [58].

obtained from multi-scale method analysis. Wang et al. [60] performed a comparative analysis on a nonlinear energy harvester between HBM and multi-scale method. The multi-scale method is applied with an excitation frequency close to natural frequency of the system. The relation between two frequencies is defined in two ways; a) $\omega = \omega_0 + \sigma\bar{\varepsilon}$, and b) $\omega^2 = \omega_0^2(1 + \sigma_1\bar{\varepsilon})$, where $\omega$ is the excitation frequency, $\omega_0$ assumed resonance frequency, $\bar{\varepsilon}$ book keeping parameter, $\sigma$ and $\sigma_1$ detuning parameters. The detuning parameter represent the nearness of excitation frequency to $\omega_0$. Results obtained from the detailed analysis show significant accuracy of HBM over multi-scale method. In case of multi-scale method, the second definition of frequency parameter in terms of eigenfrequency is found to be more efficient than a direct relation of frequency with detuning parameter in predicting acceleration response [60]. The accuracy of the solution by multi-scale method thus depends on the choice of frequency parameters.

*Phase-space based methods*

A linear system when excited with a harmonic signal the output also produces harmonics with different amplitude and phase than the input signal. In the case of a nonlinear system, the output signal does not remain purely harmonic in shape, rather it gets distorted. During vibration, additional waves are formed along with harmonic output signal. The combination of signals with different frequency components interact with each other and results in the distortion of output signal. For the small degree of nonlinearity, the effect may not be notable in the response. However, the presence of extra frequency components or distortion of response from pure harmonic signs can be visualized by observing phase-space plot of state variables. The degree of nonlinearity of breathing crack depends on the crack parameters and especially on the severity of the crack. The relationship between crack parameters and phase-space diagram is studied by Huang et al. [27]. In this work location of the crack, crack depth, etc. are varied along the length of a cantilever beam subjected to harmonic excitation, and responses are analyzed by phase-space diagram. It is shown that with the increase of crack depth or distance of crack location from free-end, phase space diagram gradually converts from a single loop to a double loop. A quasi-standard deviation method is adopted to verify the effect of crack parameters and quantify the crack depth. After a detailed numerical analysis, it is concluded that the proposed method based on the change in phase-space diagram area at cracked and healthy state of the beam is reliable only for the detection of breathing cracks rather than localization and quantification.

The identification of breathing crack is mostly carried out in the mechanical system as fatigue behavior is very common in mechanical structures. Among various damage identification methods, most of the popular methods existing in the field are based on nonlinear acoustic modulation in presence of a closing crack. The fundamental of crack-wave interaction in damage detection theory is based on the mechanism that when an acoustic signal is transmitted through the medium to be analyzed some part of it gets reflected when the crack is open and again transmitted at the time of closure of the crack. This interaction of reflected wave and input signal results in the modulation of resonating frequency and is identified by the side-band frequency in the response spectrum. This feature is utilized in the analysis of breathing crack behavior and impact of crack parameters on the response. At first, material nonlinearities are inspected by this method. Existence of super and subharmonic frequencies in each case of nonlinear investigation established this as a feature for identification of nonlinearity. Later, considering the nonlinear behavior of crack, the same features are applied by various researchers for monitoring of a system.

*Spectral analysis based methods*

The localization of breathing cracks demands a dense network of sensors for accurate localization of damage. Prawin et al. [61] proposed a novel method to detect cracks with single sensor measurement data considering the limitation of other methods. In this method, singular spectrum analysis (SSA) is performed twice. At first, dominant linear components are isolated from the spectrum and then FFT is applied on residual responses to obtain hidden harmonic components of the previous response suppressed

by comparatively higher magnitude of linear one. The nodes associated with zero-curvature or zero strain energy under swift-sine excitation with varying frequency band or single-tone harmonic excitation with different frequency-step size is taken as the primary step of breathing crack identification in this method. The zero-curvature is calculated from Eq. (39).

$$\frac{d^2x}{d^2s} = \frac{x_{i+1} - x_i + x_{i-1}}{\Delta s^2} \tag{39}$$

In Eq. (39) $x$ is the displacement, and $\Delta s$ is the spacing between two consecutive nodes along the length of the beam. The method is found to be robust even under the presence of noise with limitations of applicability in only beam members. It is also required to apply a parameter identification process to correctly identify the healthy state of the model. The selection of the frequency band is the most critical step of this model. A general spectrum analysis also suffers from different noises . The sensitivity of conventional spectrum analysis to measurement or other sources of noise is rectified by inducting a new method cyclic spectral analysis proposed in the work of Prawin and Rao [62]. Unlike spectral analysis, the special correlation-based damage indicator can identify and localize cracks without any specific cyclic excitation frequency [63]. Asymmetry in the two halves of the harmonic response in the presence of breathing crack is utilized by Yan et al. [25] for the detection and qualitative comparison of breathing crack. In this method, acceleration or displacement time-history responses are first separated into two regions; positive and negative cycles. The power spectral density (PSD) of the response for two sides of the zero axis is performed separately. The difference in natural frequency values obtained from PSD of each region of response indicates the presence of breathing crack. In practical scenario, this difference may be too small to differentiate from the effect of noise. If the analysis is performed with ambient excitation data having frequency ranges far from the natural frequency of the system, harmonics will not be excited and breathing crack identification method may fail.

The system identification alone may not fulfill all four levels of SHM defined by Rytter [64]. Consequently, beside the application of nonlinear system identification techniques, several other vibration based methods have also been developed to analyze the effect of breathing cracks on the dynamic behavior of the system. Nandi and Neogy [65] analyzed the frequency spectra of a cantilever beam with an edge crack. It has been observed that the integer multiple of forcing frequency appears in the spectra when the system is cracked and vibrated under harmonic excitation. This type of phenomenon occurs due to interaction of different frequency waves generated at the time of vibration as a result of change in stiffness. It is also seen that when the structure is vibrated at $\frac{1}{2}$ of the natural frequency of the system, the amplitude of the second harmonic is notably high. Even harmonics are also found stronger in magnitude than odd harmonics in case of beam with breathing crack. With the decrease of crack depth, odd harmonics become weaker. It is because, at a mild crack state, only asymmetric behavior of breathing crack over a period of time becomes more pronounced than other effects. This observation is considered as one of the identification features of nonlinear cracks. The beam is also analyzed with imperfect support at fixed end to differentiate the effect of breathing crack and defective support in the output response. Both of them display close behavior in terms of harmonics generated in the frequency spectrum. In many cases, it has been found that several higher harmonics remain hidden or suppressed by the effect of external noises. To enhance those hidden higher harmonics, quadratic Teager-Kaiser energy operator (Q-TKE) is used by Cao et al. [66]. The application of the Q-TKE operator reveals the energy modulation effect of nonlinear crack. It further increases the efficiency of the detection of breathing cracks. Sinha et al. [67] incorporated local flexibility around crack in the modeling. The flexibility term includes size of crack in the equation and thus could estimate severity of damage in terms of crack depth. In another work, Karthikeyan et al. [16] used an iteration technique to converge the solution to probable location and size of the crack. In this study, at first, natural frequency of the cracked member is measured. The frequency vs discretized element number along the length of the beam is plotted using the estimated response of the finite element model and assumed crack depth. The assumption about the initial location is then fixed by the interaction of frequency vs element plot and natural frequency obtained from the experiment. The concept of fracture mechanics is then borrowed to calculate equivalent crack depth for selected locations. Newton-Raphson iterative method is further used to converge to the equivalent crack depth value by minimizing the difference between theoretical and experimental flexibility coefficient values. With this equivalent crack depth, the crack location is again extracted from the plot of frequency vs beam element. Previous steps are repeated till the equivalent crack depth does not match the assumed crack depth with sufficient tolerance. The accuracy of this method depends greatly on the finite element modeling and associated measured responses. It is thus vulnerable to measurement noises which are inevitable in practical problems and thus may pollute the result.

## Identification of breathing crack by acoustic and vibro-acoustic based methods

Acoustic based methods are considered as one of the superior technology in the detection of micro cracks. High sensitivity to micro-crack, ability to inspect a larger area within the shortest time-frame, requirement of less number of sensor arrays are some of the advantages of acoustics based methods. However, for reliable implementation an accurate wave-propagation modeling, advanced signal processing, robust measurement of wave parameters etc. are required to be addressed. Detection of breathing crack depends on the modulation of incident signal by the presence of crack. The opening and closing mechanism of crack induce nonlinearity is quantitatively measured by the index proposed in the work of Hong et al. [68]. The stress transferred mechanism at different states of the crack is shown in Fig. 4. This transfer of energy between two contact surfaces also explains the transfer of energy from the primary resonant component to harmonic frequencies [69]. The nonlinear index is defined by equation of motion of nonlinear guided wave which is given as Eq. (40).

$$\rho \frac{d^2x(s,t)}{dt^2} = \frac{d\bar{\sigma}}{ds} \tag{40}$$

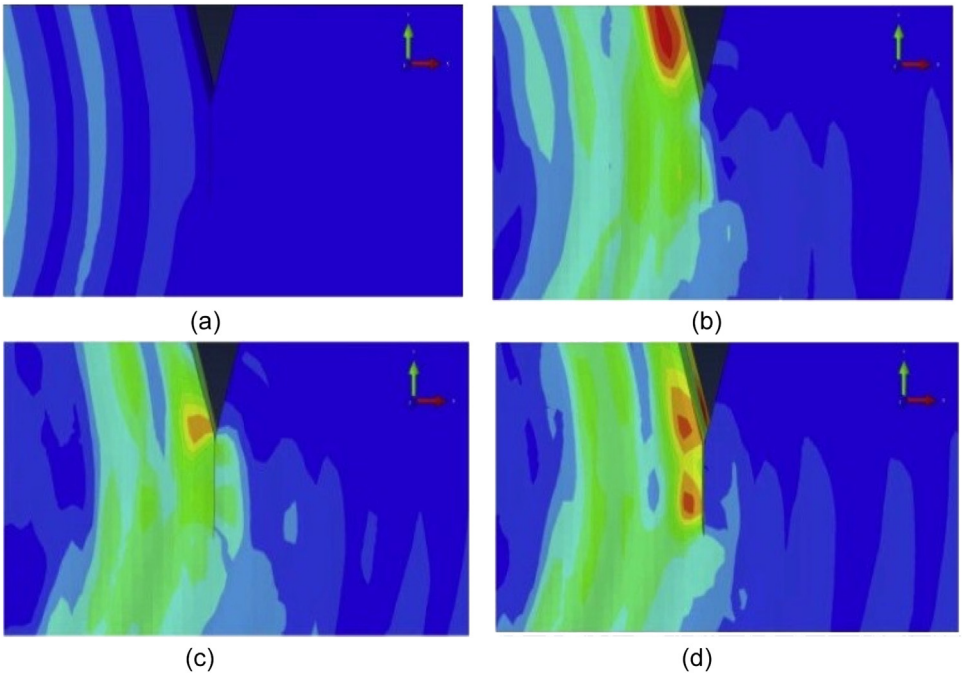


**Fig. 4.** (a) Ultrasonic wave approaching open crack, (b) stress transferred initiated at the partially closed cracked surface, (c) increase in stress transfer between two contact surfaces with the closure of crack, and (d) stress transfer discontinued at fully open state of crack [68].

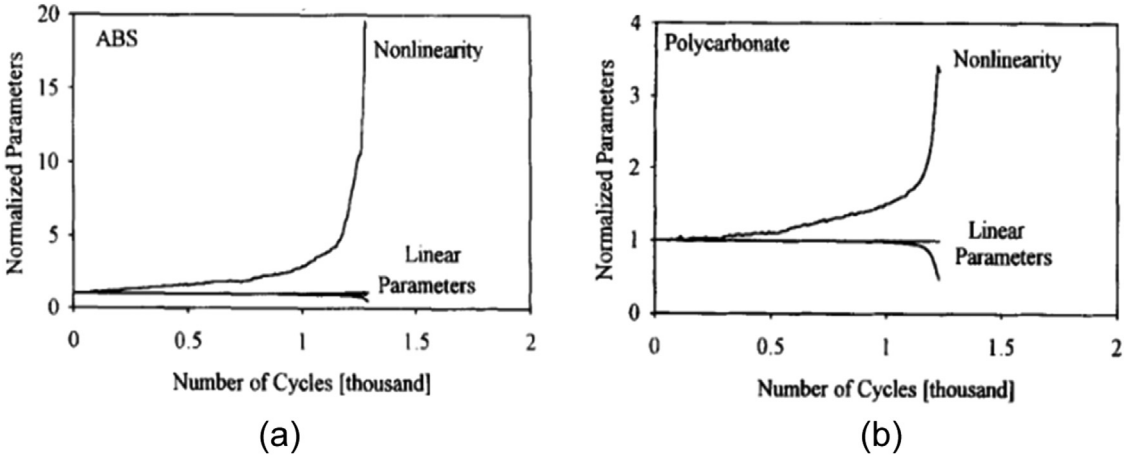


**Fig. 5.** Linear and nonlinear parameter variation for (a) ABS polymer, and (b) polycarbonate [70].

$x(s,t)$ is the displacement of wave-particle at time-instant $t$ and space $s$. $\rho$ is the material density and $\bar{\sigma}$ is stress-tensor. The solution of wave-particle derived from Eq. (40) can be represented as,

$$x = \bar{A}_1 cos\left(\bar{k}s - \omega t\right) + \bar{A}_2 \cos\left(2\bar{k}s - \omega t\right) \tag{41}$$

In Eq. (41), $\bar{k}$ is the wave number, $\omega$ is the excitation frequency, and $\bar{A}_1$, $\bar{A}_2$ are magnitudes of fundamental mode at first harmonic $\omega$ and second harmonic $2\omega$, respectively. The index thus introduced to define the change of nonlinearity is expressed as Eq. (42).

$$\bar{\beta} = \frac{\bar{A}_2}{\bar{A}_1^2} \tag{42}$$

Nagy [70] experimentally investigated the sensitivity of microscopic degradation of material to the generation of nonlinearity. The experiment performed on a ABS polymer and polycarbonate with constant-strain dynamic excitation is shown in Fig. 5(a) and (b). The variation of linear and nonlinear parameters displays the significance and high sensitivity of nonlinear characteristics in presence of fatigue damage.

This further stimulates application of different nonlinear features in the identification of breathing crack. Hayes and Rivlin [71] studied propagation of Rayleigh surface wave in a semi-infinite plate with analytical equations. In different studies, decaying of Rayleigh wave is found to vary exponentially with the depth of medium. It thus limits the application of Rayleigh wave primarily to surface or near surface fault investigation. Kawashima et al. [72] investigated the application of second harmonic of Rayleigh wave in the detection of surface crack both numerically and experimentally. The result shows that amplitude ratio of second and first harmonic increases with the increase in crack depth. The efficiency of second and third harmonic generation is explored by Yuan et al. [73] through numerical simulation of Rayleigh wave interaction with surface crack. The result exhibited a linear increase in second harmonic generation efficiency with crack depth upto $0.25\lambda$; where $\lambda$ is the wavelength of incident Rayleigh wave. Crack depth greater than $0.5\lambda$ limits the energy of Rayleigh wave to a narrower region near surface. Therefore, the crack depth shows little influence to generation of higher harmonics beyond $0.5\lambda$. This observation indicates the limitation of Rayleigh wave based method in determination of severe damage with greater crack depth. Xu et al. [38] considered both surface and subsurface cracks to develop analytical solution of stress and displacement field induced by the propagation of Rayleigh wave. A pseudo force equivalent to the difference of normal stress on the forward adjacent surface of crack at closed and open states is assumed to illustrate the mechanism of second harmonic generation. This force is further decomposed into two equivalent force components of equal magnitudes that are half of the magnitude of Rayleigh wave. One of the equivalent force components at frequency $2\omega$ is considered as the source of second harmonic generated by interaction of incident Rayleigh wave of frequency $\omega$ and existing breathing crack. Expressing this as stress tensor in elastodynamic reciprocity theorem, an analytical expression to compute second harmonic magnitude of Rayleigh wave is formulated. For the evaluation of breathing crack initiated at an angle with surface of waveguide, coordinate of the proposed explicit expression needs to be transformed accordingly to quantitatively evaluate inclined or parallel fatigue crack with similar analytical solution of vertical crack.

On the contrary to Rayleigh wave, Lamb wave has long range propagation capability. Hence, it can be utilized to interrogate a larger area than Rayleigh wave. However, till 20th century experimental realization of Lamb wave for damage evaluation was difficult due to its multi-mode dispersion property. The propagation of Lamb wave is governed by the Naiver's displacement equation with traction free surface as boundary condition. It is described by dispersion curve which plots phase/group velocity against excitation frequency. The equation of symmetric and anti-symmetric equations of Lamb wave are respectively expressed as [74],

$$\frac{\tan qh}{\tan ph} = \frac{4pqk^2}{\left(q^2-k^2\right)^2} \tag{43a}$$

$$\frac{\tan qh}{\tan ph} = \frac{\left(q^2-k^2\right)^2}{4pqk^2} \tag{43b}$$

where, $h$ denotes half thickness of a thin plate and $k$ is wave number. The term $p$ and $q$ in Eq. 43(a) and (b) are defined by the longitudinal velocity $v_l$, velocity of shear wave $v_s$ and angular frequency $\omega$ as shown in Eq. (44).

$$p^2 = \frac{\omega^2}{v_l^2} - k^2;\ q^2 = \frac{\omega^2}{v_s^2} - k^2 \tag{44}$$

Due to multi-mode dispersion property evolved from the frequency equations (Eqs. 43(a) and (b)) which are combinations of real, pure imaginary and complex roots, selection of ideal mode for Lamb wave based damage detection becomes an important objective of research [74]. Deng [75] analyzed the generation of second-harmonic lamb wave by modal approach. Later, in 2005 Deng et al. [76] conducted an experiment (Fig. 6(a)) on a thin (1.85 mm) aluminum sheet to correlate magnitude of generated second harmonic with Lamb wave dispersion. It is observed that with the increase in propagation distance second-harmonic of Lamb wave mode grows linearly. However, the cumulative growth of second harmonic is observed when fundamental mode of lamb wave is exactly equal to double frequency lamb wave mode (DFLW). The result can be interpreted from dispersion curve of Fig. 6(b). It can be seen, S2 and A2 mode of lamb wave intersect with symmetric DFLW components at a frequency line denoted by L. The intersection point marked by F0 defines the criteria for generation of second-harmonic. This observation leads to the selection of fundamental modes in many of the further works. Zhao et al. [77] studied the effect of micro-crack on the nonlinear Lamb wave mode with S0 and A0 modes. S0 mode of wave does not appear in the dispersion curve of an undamaged member. The condition for the generation of second harmonic in S0 mode of lamb wave is demonstrated in this work. From Fig. 7, one can observe that change of S0 mode in lower frequency zone is minimum than other modes. The criteria of same phase velocity for DFLW and fundamental wave thus can be more easily achieved with S0 mode than other modes of Lamb wave. Further, the location of micro-crack is determined by analyzing the reflected wave. To measure the extent of fatigue crack, a framework is presented by Kundu et al. [78] with a second-order reflection index.

The additional stress developed by the interaction of probing wave and crack acts as the source of scattered wave in a damaged structure. In this framework, modal decomposition method is exploited to scrutinize opening and closing states of crack. It is shown that during the closed state of crack displacement field of adjacent surfaces of crack are similar, while it deviates when crack is open. The transmission of wave through crack and scattering at the time of open state is the reason behind this. Further, variational principle is applied to analyze the wave generated from the crack-wave interaction. A non-dimensional nonlinearity index which is the ratio of displacement induced by crack-induced wave at second harmonic frequency and displacement induced by incident wave is proposed to correlate with damage severity. Though, numerically performance of this method is validated with a great degree of accuracy, the assumptions considered in this study may find difficulties in simulating actual fatigue crack behavior. The effect on

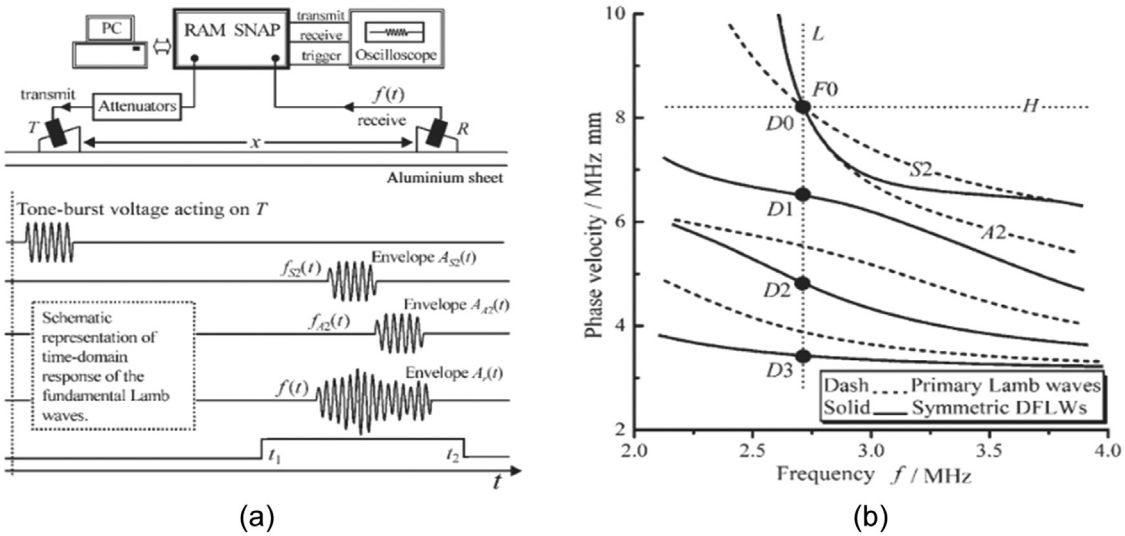


**Fig. 6.** (a) Experimental set up for the investigation of Lamb wave, and (b) Dispersion curve of fundamental mode of lamb wave and double frequency Lamb wave [76].

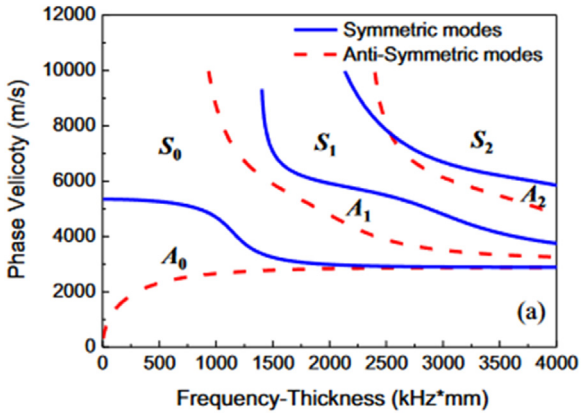


**Fig. 7.** Dispersion curve of different modes of Lamb wave [77].

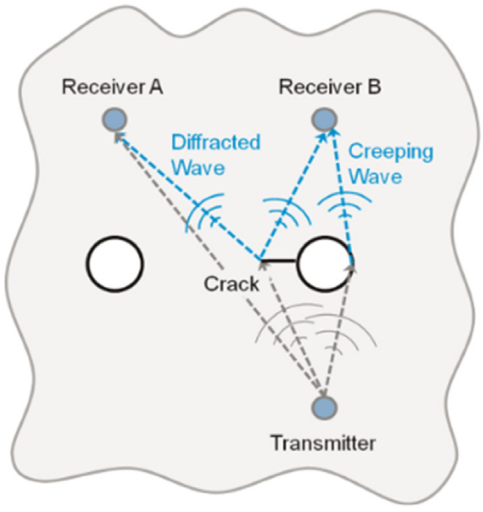


**Fig. 8.** Scattering of wave after interaction with breathing crack [31].

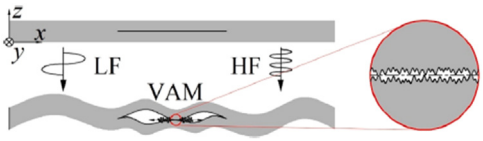


**Fig. 9.** Mechanism of vibro-acoustic method based damage detection [83].

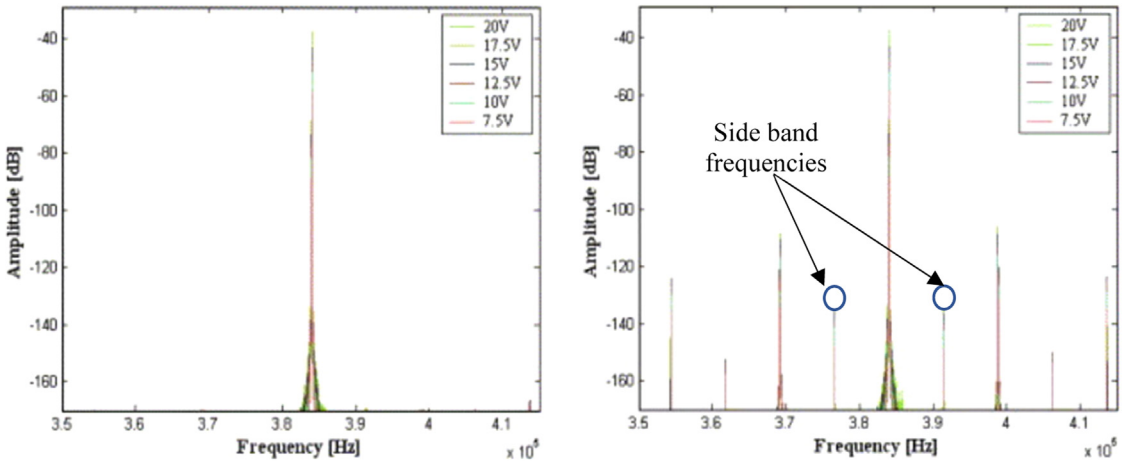


**Fig. 10.** FFT of undamaged and damaged specimen subjected to high frequency excitation [81].

Lamb wave propagation interfering with a breathing crack at the vicinity of bolt hole as shown in Fig. 8 is experimentally analysed by Cho and Lissenden [31].

A closed-form solution based on elastodynamic reciprocity theorem is also derived by Xu et al. [37] to calculate the magnitude of second-harmonic generated by Lamb wave propagation. Accounting this magnitude, a damage indicator linearly proportional to crack depth is established after numerical validation with analytical model of damage severity estimation. Nonlinear wave mixing technique using fundamental mode S0 is employed by Jingpin et al. [79]. The sideband frequency generated by nonlinear wave mixing is correlated with the size of micro-crack by performing an experiment on a plate with different micro-crack length. Nonlinearity index ($\bar{\beta}_m$) proposed in this study in terms of amplitude of sideband at sum frequency of excitation ($\bar{A}_{f_1+f_2}$) can be defined as,

$$\bar{\beta}_m = \frac{\bar{A}_{f_1+f_2}}{\bar{A}_1 \bar{A}_2} \tag{45}$$

Acoustic nonlinearity parameter given in Eq. (45) considering side band frequency shows a monotonic relationship with the length of micro-crack. Thus, amount of damage can also be assessed by the measurement of nonlinear Lamb wave mixing. Along with detection and estimation of damage severity, information about orientation of originated crack is important to predict the growth as well as for the purpose of prognosis. Wang et al. [34] addressed this problem by finding out a unique scattering effect of contact acoustic nonlinearity at the inclined surface of crack.

Though sensitivity of crack-wave interaction has been proved to be superior through numerous simulations and experiments, effect of ambient disturbances or environmental factors are inevitable in its practical application. The scattered wave from the surface of crack is evaluated further to detect the presence of crack.

Vibro-acoustic methods have also been receiving much attention now-a-days to identify and measure the severity of fatigue damage. Principle of vibro-acoustic method is based on the analysis of modulated output response of two excited signal applied on the damaged structure. It is graphically depicted in Fig. 9. A strong effect of nonlinear motion on acoustic wave propagation is observed with subharmonic generation by Solodov et al. [30]. Donskoy and Sutin [80] developed two vibro-acoustic methods- (a) based on modulation of sinusoidal probe wave, and (b) modulation of impact vibration signal. Both of these methods established notable correlation between side band frequency components and presence of contact type crack. At undamaged state, low frequency vibration and ultrasound wave appear separately in the frequency spectrum of response.

In presence of damage, these two frequency components interact together and generates side band frequency as an indicator of damage. The separation of nonlinear signal components from probe signal shows the advantage of its application in the evaluation of breathing type of damages. The appearance of side band frequency is experimentally validated by Meo and Zumpano [81]. In this study a clear distinction between an undamaged plate response and impact damage induced nonlinearity is explored [Fig. 10]. Klepka et al. [82] implemented a vibro-acoustic method for the experimental investigation on fatigue crack detection. Modulation of wave at low and high frequency acoustic excitation by different crack modes are examined in this work. In each vibration mode, interaction of wave and crack edge has shown significant effect on wave modulation. It is also observed that the modulation of wave

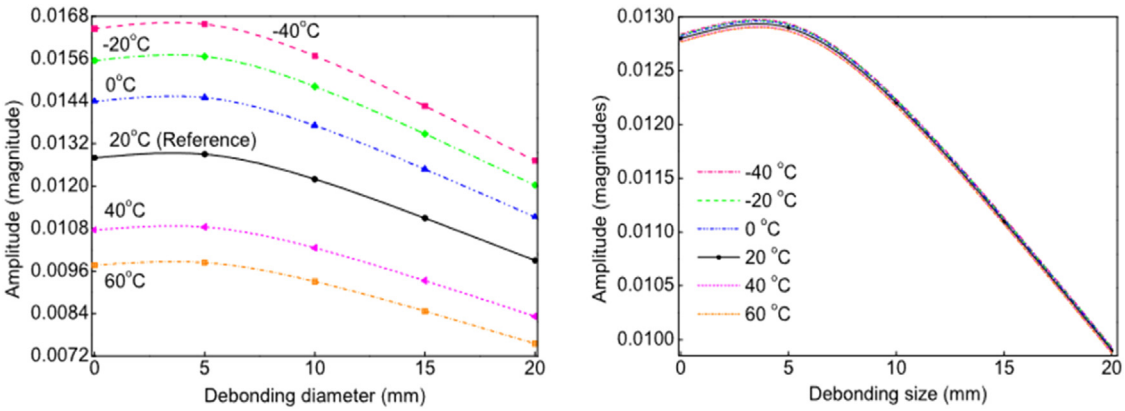


**Fig. 11.** Effect of temperature variation on A0 mode amplitude of Lamb wave (a) before applying correction factor, and (b) after applying correction factor [84].

in presence of fatigue crack can be engendered by weak-stain field of material even if crack is not open. Thus, even at closed state of vibro-acoustic method successfully detects crack. Breathing mechanism facilitates in amplifying the intensity of modulation which is measured as the ratio of sum of spectral amplitude at pair of side band frequency and spectral amplitude at acoustic frequency. This method is further extended to identify delamination of plate by He et al. [83]. The variation of second harmonic in presence of breathing crack is studied by Lee and Lu [3] to isolate nonlinear crack from other sources of nonlinearity. The reduction of nonlinear index during vibration relative to stationary condition is projected as a signature of crack. One of the most complicating factor in the application of vibro-acoustic mechanism is dependence of wave modulation on the excitation frequency.

Incorporation of nonlinear features of guided wave is also increasing at a faster rate towards its implementation in earlier prediction of damage parameters. However, noises emerged from other sources than flaws in a material or system may also present similar characteristics in the captured signal as fatigue crack. Hence, a series of researches are being conducted accounting the effect of environmental or other sources of nonlinearity.

Sikdar et al. [84] proposed a novel technique to compensate temperature effect on Lamb wave propagated through a debonded composite structure. Efficiency of the method in eliminating the temperature effect is shown in Fig. 11(b). More detailed review on the effect of environmental factors and their mitigation techniques are described in a review by Gorgin et al. [85]. The summary of the methods reviewed in this section is presented in Table 1 to categorically extract their salient features.

## Modeling of breathing crack

Accurate modeling for the simulation of real crack behavior is the first step toward the exact solution of nonlinear vibration. Various methods have been undertaken in the past to model the breathing behavior of cracks by analytical, numerical, or experimental models. In this section, each of the modeling techniques is separately reviewed. The analytical model explains the behavior of breathing cracks in a mathematical form. The numerical analysis summarizes the procedure of opening-closing modeling of a crack using some established software packages. The experimental models on the other hand give insight about the practical procedures for simulating closing crack behavior. The material, physical and geometrical properties are also provided along with the description of modeling technique. It is to facilitate researchers in validating the results of the proposed method or to identify a more accurate procedure for the simulation of the original behavior of the cracked member.

### *Theoretical modeling of breathing crack*

Breathing crack is a phenomenon where a crack in a member opens and closes at a certain frequency under excitation force or vibration. However, in practical situations, two surfaces of a crack may not completely close due to the presence of surface roughness. Thus, actual area of contact is less than the area of cross-section at fully closed state. This type of contact is generally not considered in the analytical model for simplicity. Some of the efforts are made in the past to successfully describe this mechanism with different assumptions in modeling. Gasch [86] proposed ‘hinge model’ for the simulation of opening-closing mechanism of crack in a rotor shaft. Stiffness of the member is expressed as a function of crack angle. In this model, the state of crack is defined as either open or close. The transition between two states of crack is not considered in this model. This drawback is resolved in the work of Mayes and Davies [90] where a relation is established between change in stiffness and crack depth or angle. The difference in the mathematical approach can be explained by the following Fig. 12. It can be seen in the figure that opening-closing function is having only two values 0 and 1 as per the modeling of Gasch [86] corresponding to open and closed states respectively. Mayes and Davies modified this model by considering a periodic variation of crack closure with functional values between 1 and 0 [87]. At the time of slow rotation of shaft due to its own weight, the crack surface opens and closes. The angle of crack changes with the rotational angle. It

**Table 1**
Summary of nonlinear damage identification methods.

| Methods reviewed | Fundamental theory | Signal type | Damage type | Method | Advantages | Limitations |
|---|---|---|---|---|---|---|
| GFRF | Expansion series | Vibration | Breathing crack | Theoretical | Directly operates on time-domain response | Multi-dimensional function |
| HOFRF | | | | | Effective in measuring higher frequencies of vibration response | Applicable for purely harmonic excitation |
| NOFRF | | | | | One dimensional function, isolates frequencies originated from nonlinear response | Less sensitive to small crack induced changes |
| OFRF | | | | | Explicit connection between nonlinear parameters and output frequency response | Not applicable for nonlinear systems which generate subharmonics and chaos |
| Coherence based method | Higher-order statistics | | | Numerical | Noise resilient | Requires long time data record |
| Harmonic balance method | Fourier series | | | Numerical | Easier to operate | Suitable for weakly nonlinear system |
| Runge-Kutta method | Iteration method | | | Numerical | Better accuracy | Time-consuming method |
| Regular perturbation | Perturbation method | | | Theoretical | Analytically express the influence of change in system parameters on the response | Inclusion of secular term diverges the solution |
| Phase space based method | Graphical method | | | Theoretical | Minimum computation | Noise sensitive |
| Spectral analysis based method | Fourier Transformation | | | Theoretical | Robust to noise | Performs better within a selected frequency band |
| Rayleigh wave based method | Crack-wave interaction | Acoustic and Vibro-acoustic | | Theoretical | Advantageous for the detection of surface crack | Primarily applied on structures with simple geometry |
| Lamb wave based method | Crack-wave interaction | | | Theoretical | Capability to investigate comparatively larger area | Multi-mode behavior, applications limited to thin member |

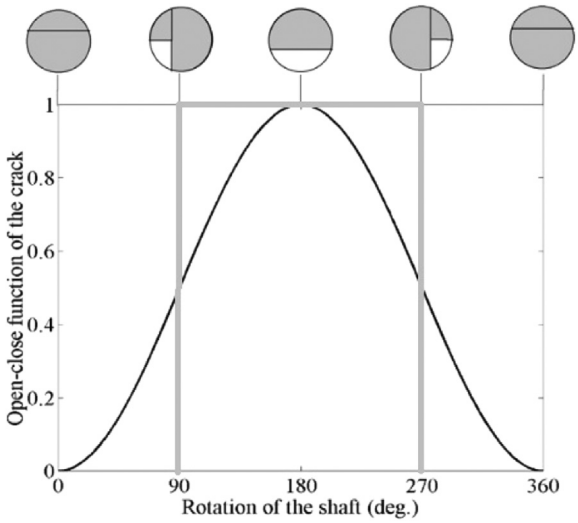


**Fig. 12.** Opening-closing model of crack [86].

is reported in the study of Penny and Friswell [88], that for small crack depth, the bi-linear mechanism of hinge model is a good approximation.

When the crack depth is deep, Mayes and Davies model well simulates the behavior. The stiffness value calculated from the hinge model is calculated as Eq. (46).

$$K = \begin{bmatrix} k_{\xi}(\Theta) & 0 \\ 0 & k(\Theta) \end{bmatrix} \tag{46}$$

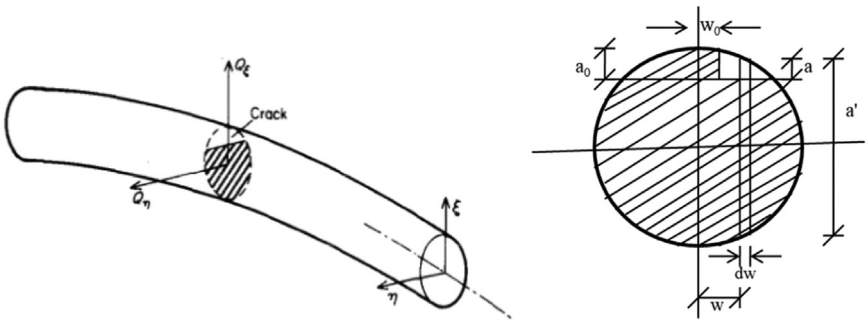


**Fig. 13.** Geometrical coordinates and cross-section of a rotor shaft [89].

Here, $k_\xi(\Theta)$ and $k(\Theta)$ are functions of angular rotation of shaft. $\xi$ and η are rotation coordinates. The time-variant stiffness is defined by Eq. (47) in the Gasch model [86].

$$k_\xi(\Theta) = \begin{cases} k_c & -\frac{\pi}{2} \le \Theta < \frac{\pi}{2} \\ k_{\xi 0} & \frac{\pi}{2} \le \Theta < \frac{3\pi}{2} \end{cases}$$

$$k(\Theta) = \begin{cases} k_c & -\frac{\pi}{2} \le \Theta < \frac{\pi}{2} \\ k_0 & \frac{\pi}{2} \le \Theta < \frac{3\pi}{2} \end{cases} \tag{47}$$

In Eq. (47), $k_c$ is the stiffness of the member at fully closed crack state. $k_{\xi 0}$ and $k_0$ are stiffness along two directions of rotational coordinates. In Mayes and Davies work [87], instead of expressing the equation with two limiting conditions as a function of rotation of the shaft, stiffness values are defined by the cosine function (Eq. (48)).

$$k_\xi(\Theta) = \frac{1}{2}\left(k_c + k_{\xi 0}\right) + \frac{1}{2}\left(k_c - k_{\xi 0}\right) cos\ \Theta \tag{48}$$

This model has been employed in many studies [83] for the analysis of breathing crack behavior and its impact on the response. Jun et al. [89] later utilized the concept of fracture mechanics to derive direct and cross-coupled stiffness of a vibrating member. The behavior of a rotating shaft with breathing crack is complex in nature. It is due to the interaction between direct and cross-stiffness in the presence of unbalanced mass and when self-weight of the shaft is comparatively dominant in the stress contribution to the member. The stiffness matrix calculated as per this model is given in Eq. (49).

$$K = \begin{bmatrix} k_\xi(\Theta) & k_\xi(\Theta) \\ k_\xi(\Theta) & k(\Theta) \end{bmatrix} \tag{49}$$

The cross-coupling stiffness is only obtained at partially open and closed states of crack when stiffness along two directions of rotation coordinates participate. In reality, this coupling effect occurs when a crack is deep in length. For vibration with any one state of crack either open or closed, the cross-coupling stiffness turns zero and the matrix becomes similar to that of Gasch [86] model. In Jun et al. model [89], it is assumed

$$K_{Q\xi} = \sigma_\xi(w)\sqrt{\pi a} f\left(\frac{a}{a'}\right)$$

$$K_Q = \sigma(w)\sqrt{\pi a}\ f'\left(\frac{a}{a'}\right) \tag{50}$$

that due to large length of shaft than a' (Fig. 13), the stress intensity factor $K_{Q\xi}$ due to force $Q_\xi$ along $\xi$ direction is approximately equal to the bending stiffness. Similarly, for force $Q$ along transverse direction η, stress intensity factor (SIF) $K_Q$ is given in Eq. (50). $\sigma$(w), $f(\frac{a}{a'})$ and $f'(\frac{a}{a'})$ are obtained from the established empirical formula. The total stress-intensity factor of the member is the summation of individual SIF given in Eq. (50). The total deflection of the member is then calculated by combining the deflection of non-cracked section and excessive deflection due to crack. The total deflection is expressed by the form given in Eq. (51).

$$\Delta_\xi = Q_\xi C_1 + Q C_2 \text{ and } \Delta = Q_\xi C_3 + Q C_4 \tag{51}$$

Where $C_1$, $C_2$, $C_3$ and $C_4$ are flexibility coefficients. The final values of direct stiffness and cross-coupling stiffness w.r.t rotational coordinates $\xi$ and η are computed as in Eq. (52).

$$k_\xi = \frac{C_4}{C_1 C_4 - C_2^2};\ k_\xi = k_\xi = \frac{-C_2}{C_1 C_4 - C_2^2};\ \text{and } k = \frac{C_1}{C_1 C_4 - C_2^2} \tag{52}$$

In some research, influence of open crack on bending stiffness *EI* is analyzed and an equivalent value of *EI* in the presence of a crack is proposed (Eq. (53)).

$$EI = EI_0 f_1(x);\ \text{where } f_1(x) = 1 - \emptyset_1 e^{-\alpha|x - x_c|/d} \tag{53}$$

Wei and Shang [90] combined the opening and closing state stiffness value with a new function to describe breathing crack with a single Eq. (54).

$$EI = EI_o\left(1 - \frac{1}{2}\left(1 - f_1(x)\left(1 - sgn\left(\frac{d\Psi}{dx}|x = x_c\right)\right)\right)\right) \tag{54}$$

$\Psi$ is the angle of rotation of the cracked section. Joglekar and Mitra [91] used inverse of additional compliance ($C_T$) to represent opening state of crack. The reduction of stiffness due to open crack state is represented by introducing a rotational spring of equivalent stiffness. The value of additional compliance $C_T$ is calculated as Eq. (55).

$$C_T = \frac{72\pi}{Ebh^2} f\left(\frac{a}{h}\right) \tag{55}$$

Here, $E$ = Young's modulus, $b$ = breadth of cross-section, $h$ = thickness of member, and $a$ = depth of breathing-edge crack. Following the switching method of Gasch [86] on rotating shaft, Chatterjee [23], Chu and Shen [17] analyzed a single DoF system and cantilever beam respectively as bi-linear oscillators with a breathing crack. The equation of motion of the system is separately defined for two regions; one for tension, and another for compression. Nguyen [92] expressed stiffness of breathing-crack members in terms of curvature (Eq. (56)).

$$K = k_c + \frac{1}{2}(k_c - k_o)\left[1 + \frac{\emptyset''}{\emptyset''_{max}}\right] \tag{56}$$

$\emptyset''$ is curvature of the member. The normalized ratio of curvature may result in singularity if absolute value is not used. This method of modeling breathing-crack scraps the requirement of open-close frequency which is generally assumed for analysis and difficult to measure in other cases. Rezaee and Hassannejad [24] proposed an amplitude-dependent function for time-varying stiffness. The local stiffness value at open and closed states at a point and its corresponding amplitude are related by the following Eq. (57).

$$K = k_c + \frac{1}{2}(k_c - k_o)\left[1 + cos\left\{\frac{\pi}{2}\left[1 - \frac{A_o^2 + A_o^2}{A_o A_c(A_o - A_c)}A + \frac{A_o + A_o}{A_o A_c(A_o - A_c)}A^2\right]\right\}\right] \tag{57}$$

$A_o$ and $A_c$ are amplitude of a point at fully open and closed states of crack, whereas A is the amplitude of the same point on the member. Most of the analytical models have used direct integration technique or 4th order Rungee-Kutta method for the solution of nonlinear equations [25]. In another study, Ruotolo et al. [19] expressed the closing crack function in the form of Fourier series. The equation of motion incorporating cracked function is given in Eq. (58).

$$m\ddot{x} + c\dot{x} + \left(k - \Delta k\bar{f}(t)\right)x = P(t) \tag{58}$$

$\bar{f}(t)$ is a closing crack function, and $\Delta k$ is reduction in stiffness of the cracked cross-section when crack is fully open. The cracking function $\bar{f}(t)$ is defined in Eq. (59).

$$\bar{f}(t) = \frac{1}{2} + \frac{2}{\pi}\cos(\omega t) - \frac{2}{3\pi}\cos(3\omega t) + \frac{2}{5\pi}\cos(5\omega t) + \ldots \tag{59}$$

*Numerical modeling of breathing crack in beam*

The theoretical modeling approach is cumbersome to solve a complex problem. Also, for a nonlinear problem, a closed-form solution hardly exists. Numerical methods are applied to solve this problem with the theoretical background of breathing crack modeling. In most of the cases of SHM based diagnosis, a baseline or reference state is required. However, the practical measurements of reference or healthy state response may not be available. A model-based approach is considered as one of the solutions in such cases. Various software packages are available for advanced modeling and analysis techniques. Some of the packages which have been widely used in the past for modeling of breathing crack mechanisms is discussed in this section. This is to facilitate future researchers in developing more advanced methods with greater accuracy extending the knowledge of existing techniques.

Cao et al. [93] proposed a concept of quadratic Teager-Kaiser energy (Q-TKE) to amplify the peaks of higher-order harmonic frequencies generated by the breathing mechanism which may remain hidden in the frequency spectra. The effect of Q-TKE is verified with a numerical model of steel cantilever beam with breathing crack. 'Ansys' software package is employed for the numerical modeling and simulation. Simulation of opening-closing mechanism is the main difficulty, one may face during this modeling. Every software package has limited options to model a structure with specific material properties and physical features. Hence, attaining significant accuracy with the finite element modeling within the limited software environment is a challenge. The review in the present section opens up different methods to assist in developing new model for intended purpose. In the work of Cao et al. [93], following physical parameters are considered as given in Table 2. The graphical description of the model is shown in Fig. 14. The crack is modeled by inserting two extra surfaces with zero thickness at the selected crack locations. The nodes are distributed on the cracked surface similar to the distribution of adjacent faces to form floating coincident nodes. Penalty algorithm used in this modeling ensures no penetration interaction between two cracked surfaces. A similar approach is used in another study [50] to model delamination of a cantilever composite plate of dimension 5 mm x 5 mm x 0.625 mm carbon-fiber-reinforced polymer (CFRP).

Dotti et al. [94] analyzed a thin-walled cantilever C-section (Fig. 15) with a breathing crack in 'ABAQUS'. Two types of element shell and beam are used for the finite element discretization of the beam, and results are compared. Both shell and beam models are observed to display a fair level of accuracy. To model interaction between two cracked surfaces, two types of contact definitions are used in normal and tangential directions. 'Hard' contact along normal direction allows the transfer of full pressure between two

**Table 2**
Parameters for numerical analysis of a cantilever beam with breathing crack.

| Sl. No. | Properties and parameters | Description |
|---|---|---|
| 1. | Member | Cantilever beam |
| 2. | Material | Steel |
| 3. | Section | Rectangular |
| 4. | Dimension (length × width × thickness) | 400 mm × 10 mm × 20 mm |
| 5. | Fixed end | Fixed by spanning 20 mm from the fixed end |
| 6. | Density | 7800 kg/m$^3$ |
| 7. | Elastic Modulus | 200 GPa |
| 8. | Poisson's ratio | 0.27 |
| 9. | Damping ratio ($\zeta$) | 0.1 |
| 10. | Damping type | Rayleigh Damping |
| 11. | Finite element dimension (length x width x thickness) | 10 mm x 2.5 mm x 2 mm |
| 12. | Element type | 8 node hexahedral |
| 13. | Excited force | Concentrated |
| 14. | Location of exciting force | 30 mm away from the fixed end |
| 15. | Exciting Force | 100 N |
| 16. | Excited frequency | Arbitrary |
| 17. | Location of measurement | 10 mm away from free end |
| 18. | Sampling frequency for analysis | 1000 |
| 19. | Response measured | Stead-state velocity, sampled 40 points in one period |
| 20. | Crack depth | 6 mm |
| 21. | Location of crack (distance/length) | 0.2, 0.4, 0.6, 0.8 (Each case considered separately) |
| 22. | Method used to model two-crack surface interaction | Penalty algorithm |

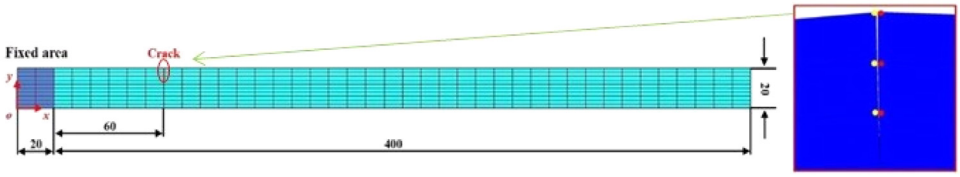


**Fig. 14.** Finite element modeling of breathing-edge-crack in a cantilever beam [93].

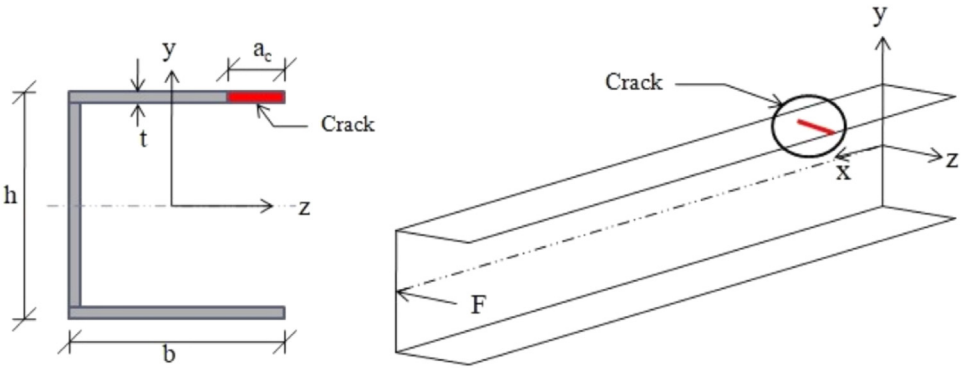


**Fig. 15.** Cross-section and longitudinal section of a thin-walled beam with breathing crack.

surfaces at the time of closed state of the crack. Thus, returns back to initial stiffness value. Contact stress is reduced to zero when two surfaces are separated at open state of crack. Along the transverse direction, 'rough' surface is opted to restrict the sliding between the surfaces at closed contact. However, defining actual roughness coefficient is practically difficult. It is also observed that modeling with beam element presented superiority in computation time over the shell model. In many nonlinear analysis, a small error in modeling may lead to a large error in time-history results by getting accumulated in a nonlinear manner at each time-steps of calculation. Hence selection of element type is also crucial for any nonlinear analysis.

The penalty algorithm in 'Ansys' has some flexibility in allowing small penetration when cracks get closed unlike 'Abaquas'. It is thus practically more realistic than 'hard' surface modeling which will produce an additional wave of impact force. Practically, surfaces adjacent to a crack may never fully open and close during vibration. If the area of cross-section that will come in contact during vibration can be defined prior to analysis, it will have more realistic approach toward the simulation of real problems.

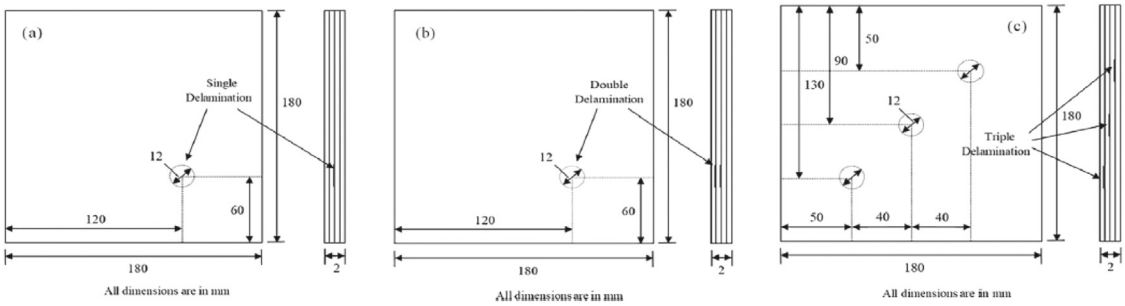


**Fig. 16.** Physical description of GFRP plate with (a) single, (b) double, and (c) triple delamination [48].

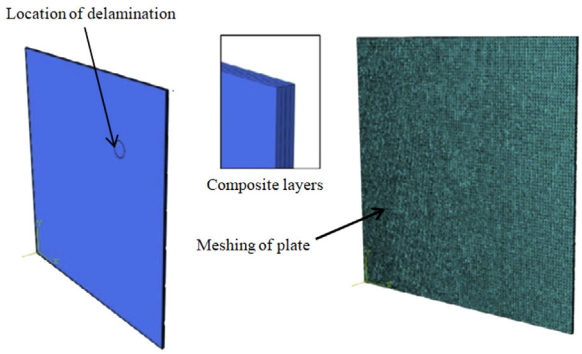


**Fig. 17.** Model of GFRP plate in ABAQUS [48].

*Numerical modeling of plate delamination*

The delamination effect of multi-layer glass-fiber-reinforced-polymer (GFRP) plates has been studied by Roy et al. [48] through numerical analysis. ABAQUS 6.14 software package has been used for this purpose. The geometrical dimension of each layer of the GFRP plate is taken as 0.18 m x 0.18 m x 0.002 m. The bond between each layer of GFRP plate is modeled by using surface-to-surface tie contact. Sliding interaction is provided between the two layers of GFRP plates at the intended section to model delamination between two layers of GFRP plate. It is shown in Fig. 16. To transmit and receive signal, nodes far from the delamination zone are selected. A MATLAB-generated chirp signal of 20 N amplitude is applied at the node created for transmitter signal. The frequency range of chirp signal should fall between local defect resonance (LDR) frequency.

A signal outside the band of LDR would not be able to excite nonlinear resonating frequencies of the member. Discretization element chosen for meshing of the plate is a 10-noded quadratic tetrahedron element. The meshed model is shown in Fig. 17. Output signal at a node is measured which is further processed for the FFT analysis and determination of bicoherence value. The delamination region is considered circular in shape with 0.012 m diameter and $2 \times 10^{-6}$ m thickness. An explicit analysis is performed to determine steady-state results with size of element and time-increment value calculated by Courant-Friedrichs-Lewy's law [95]. The application of CFL law ensures stability of the solution with assumed time steps and size of mesh elements.

*Experimental modeling of breathing crack*

An experimental model to a greater extent represents a real scenario. The development of any formulation is hence better validated with small-to-large-scale experimental modeling in the absence of real data. Many researchers look for the experimental dataset or guidance to develop a new model in order to verify their proposed methods. A short description of some of the experimental models in this review may address this problem. From the literature reviews, it has been observed that most of the studies on breathing crack problems have been performed on either rotor shafts or plates and beams. Very few studies are there on large-scale models such as shear buildings, frame structures, bridges, etc. Also, the design of an experimental set-up to initiate and propagate cracks with fatigue behavior is a very complex process.

Hence, in experimental modeling also some relaxations are made to achieve the desired behavior of the model with ease. Jiang et al. [49] experimented with an aircraft blade-shaped member made of bamboo fiber to detect fatigue cracks. A narrow slot is made on the blade and randomly vibrated with an exciter. The slot is made by cutting some portion of blade at the top with a utility knife. The whole arrangement of the test set-up is shown in Fig. 18. A forced vibration oscillator is installed with a frame to apply vertical excitation at selected node of the member. One video camera is assembled with a telescopic lens of large zooming capabilities to capture the motion of beam. The position of the camera is set in such a way that all characteristic points where the response is expected

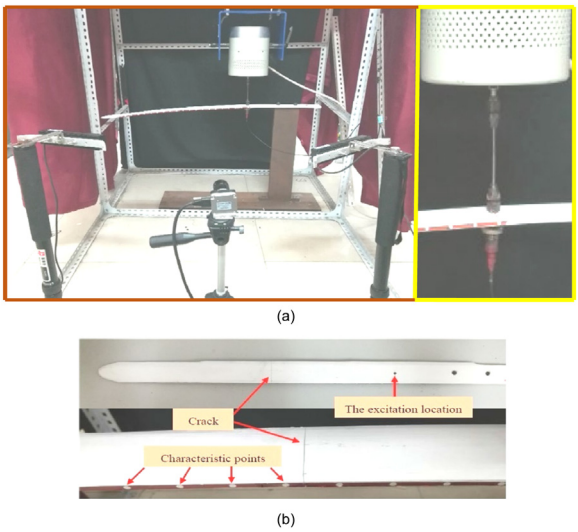


**Fig. 18.** (a) Experimental arrangement of an aircraft-wing model with forced vibration exciter, and (b) location of crack and characteristic points of the model [49].

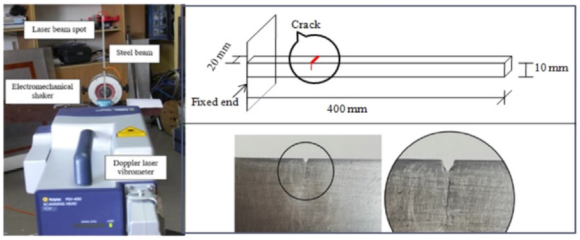


**Fig. 19.** Geometrical description of a vertical aluminum cantilever beam and experimental arrangements [96].

to be measured fall in the region of the telescopic lenses. The result of the proposed total nonlinearity index (TNLI) estimated from the response exhibits the capability of identifying even small damage with a lower degree of nonlinearity. At the same time, it verifies the presence of breathing crack with nonlinear features extracted from the system's response. However, the flexible dimension of aircraft wing model may incorporate geometric nonlinearity in the response if vibration amplitude is not controlled. It may mislead the result about breathing crack identification. Xu et al. [96] used an electromechanical shaker to apply harmonic force on a vertically held steel beam (400 mm x 10 mm x 20 mm) with a 1 mm notch near fixed end. The notch is triangular in shape. From the edge of the notch tip, a 5 mm deep crack is produced by fatigue vibration of the beam. The test setup of the beam is shown in Fig. 19. Doppler laser vibrometer is installed to measure the velocity response at the selected measured points.

The selection of the input voltage which controls displacement amplitude is an important task for the detection of nonlinearity. This small-scale model of the beam may also exhibit geometric nonlinearity by the applied harmonic force. This is the reason experiment with higher voltage is excluded from the analysis to restrict the generation of geometric nonlinearities by excessive deformations. Frequency spectra of the velocity response is applied to detect the nonlinear response by the appearance of higher harmonics. The amplitude of higher harmonics is noted to be more dominant in the acceleration spectrum than velocity. The acceleration time history is obtained from the measured steady-state velocity response. Finite difference method is adopted for the numerical differentiation of velocity to calculate acceleration response. A similar type of test setup is used by Cui et al. [97]. In place of a vertically held beam, a horizontal beam is used to record transverse vibration excited by the electromechanical shaker. Accelerometers are attached to directly record the response of selected points near the crack. Two parts of the beams are glued with each other. In the bottom part of beam a through-width crack is made. To avoid unbonding by shear between two glued beam surfaces, thickness of the top and bottom beam is kept same to amount equal deflection at the same cross-section. The arrangement of beam and shaker is shown in Fig. 20. In this experiment, as the beam is fixed horizontally, self-weight of the beam will also contribute to the response. Weight of the beam acts as a restoring force when the crack is on the upper side of the beam and in the closing state during motion. If this static gravity force overpowers the excitation amplitude of vibration, breathing behavior would not develop. To minimize the interference of gravity load, a force exciter has been used in the middle to vibrate the beam with a minimum initial deflection at the non-excited position of the beam. The stress concentration at the crack tip is ignored in this experimental model unlike the work of Xu et al. [96] which would better represent actual behavior of the cracked beam. The natural frequency of the beam is found to be 21 Hz. Hence, the excitation frequency is set close to the resonating frequency equal to 15 Hz throughout the experiment. In this method,

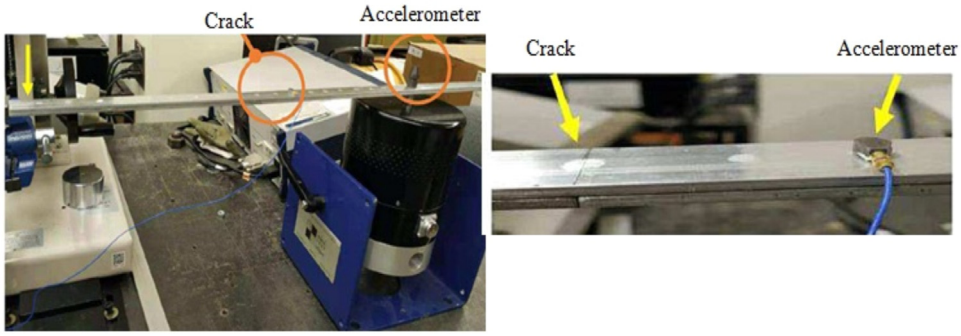


**Fig. 20.** Horizontal arrangement of beam with shaker and position of accelerometer [96].

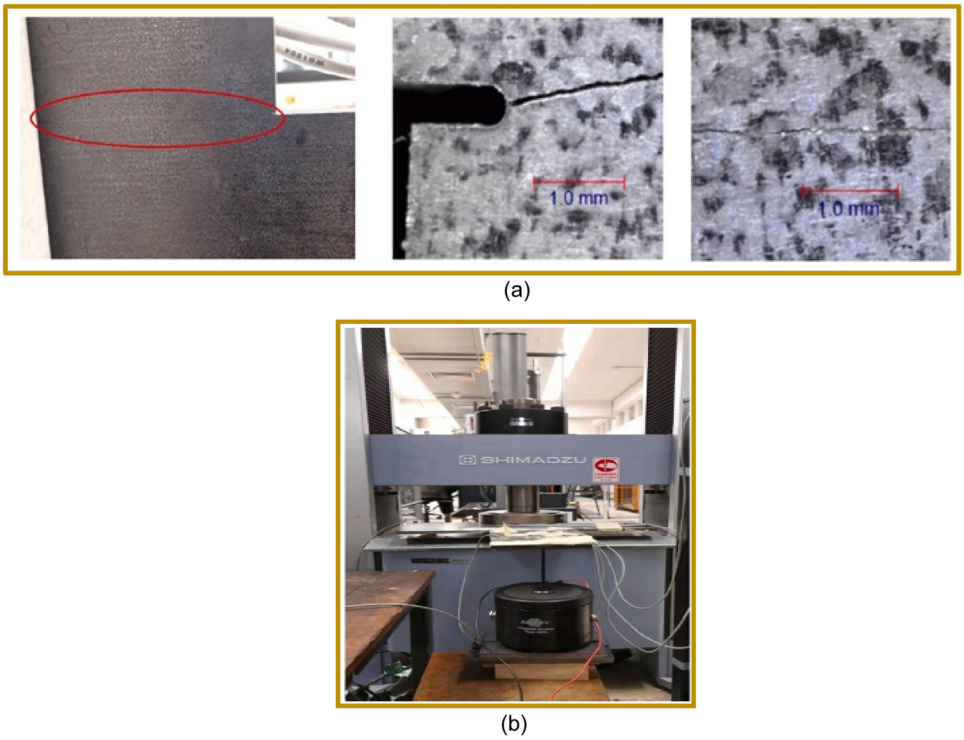


**Fig. 21.** (a) A cracked T-beam and path of crack-propagation, and (b) laboratory setup [3].

the breathing nonlinearity may get coupled with geometric nonlinearity of beam if excitation amplitude is not controlled. Lee and Lu [3] investigated a T-shape steel plate model with crack at corner between the joint of the flange and web. Tensile cyclic loading is subjected to the model with 150 MPa maximum stress and 15 MPa minimum stress. After the development of fatigue crack by 54 mm in length, the specimen is subjected to nonlinear-ultrasonic testing. The flange of the specimen is kept fixed whereas no support is provided to the web of the joist. Four sensing paths are marked on the body of the web to sense the propagation of breathing cracks. Both vibration and ultrasonic signals are then generated to examine the effect of nonlinearity on the vibration response. As the crack propagates along sensing path 4, response recorded in this path will not have any significant impact due to nonlinearity. The size of the crack is shown in Fig. 21. It can be observed that crack is wider near the crack tip and reduced gradually towards the flange edge. Also, as propagation of crack occurs along sensor path #4, response collected at any point on this path does not show any impact of fatigue crack. Response along the sensing paths #2 and #3, located away from the crack tip is analyzed here to evaluate the effect of vibration. A composite plate is investigated by Rébillat et al. [98] to determine the presence of breathing crack using nonlinear features of the system's response. The composite plates used in this study are aircraft composite fuselage. Each plate consists 16-layers of carbon-epoxy material. A network of PZT sensors is built on the plate as shown in Fig. 22. Among two plates, one plate is damaged at the center by projecting steel ball on the surface with controlled velocity. Impact of this 5 mm diameter steel ball creates local deformation on the plate surface as a mark of damage. An exponential sine sweep signal is then generated to excite the plate with frequencies $f_1 = 100$ Hz and $f_2 = 30$ Hz. The output results indicate the presence of nonlinearity even in the healthy state. Hence, with

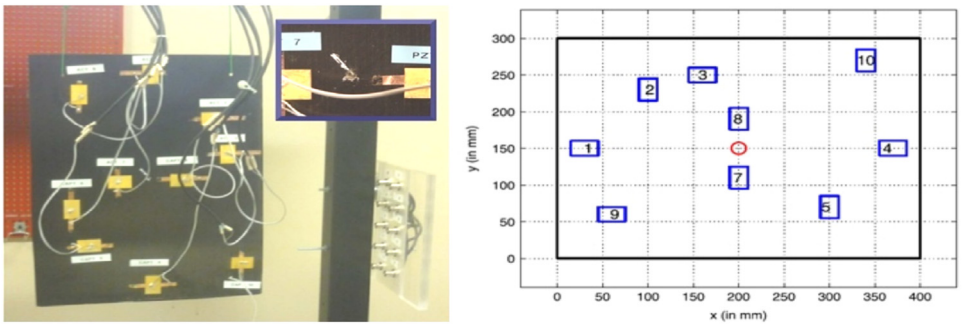


**Fig. 22.** Arrangement of accelerometers and crack position on a composite plate [98].

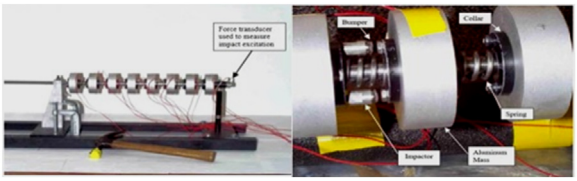


**Fig. 23.** A 8-DoF spring-mass system with contact nonlinearity [100].

**Table 3**
Parameters for experimental analysis of a plate with breathing crack.

| Sl. No. | Properties and parameters | Description |
|---|---|---|
| 1. | Geometrical shape of plate | Rectangular |
| 2. | Dimension (Length × breadth × thickness) | 400 mm × 300 mm × 2 mm |
| 3. | Damage location | Center of plate |
| 4. | Number of PZT patches | 9 |
| 5. | Dimension of patches (Length × breadth × thickness) | 30 mm × 20 mm × 0.2 mm |
| 6. | Orientation of composites | $(0^\circ, 45^\circ, -45^\circ, 90^\circ, 90^\circ, -45^\circ, 45^\circ, 0^\circ)_2$ |
| 7. | Sampling frequency | 100 kHz |
| 8. | Forcing voltage amplitude | 10 V |

this experiment it is difficult to study only the effect of breathing crack as the response of damaged plate will include other inherent sources of nonlinearity along with nonlinear behavior of the crack if present. The details of plate dimensions, placement of PZT patches, damage location, etc. are provided in Table 3. Fatigue crack in the welded joint of a girder is experimentally tested by Kong and Li [99]. A compact C(T) specimen is tested under fatigue loading. The digital image processing method is employed here to detect opening and closing of crack during fatigue cycles. All results obtained from the test collectively exhibit the breathing phenomena after data processing. Hence, in future, it could also be employed with accelerometer or other sensors to perform a nonlinear damage detection study with measured response time-history. Some experimental set up are also developed in the past to simulate a nonlinear system which can be utilized for breathing crack modeling in future. In one such work, a #8-DoF spring-mass system is developed with series of discs connected by a spring. The nonlinearity is developed in this model by placing a bumper (Fig. 23) between two masses to restrict movement of attached masses between damaged spring and enable collision. This experimental model is developed for validation of nonlinear system identification technique.

The same arrangement can be used to represent fatigue cracks with variable stiffness. To achieve this the solid bumper can be replaced with a spring. Stiffness of bumper spring should be selected in such a way that after collision the total stiffness (damaged spring + bumper spring) will be equal to the stiffness of spring at undamaged position. However, in this way, the axially vibrated system could not replicate gradual closure of the crack. Rather, the equation for this system will follow the theoretical model of Gasch [86]. Similar arrangement is made in a #4-DoF frame model. An inverted suspended stringer is attached to the bottom of top floor and an obstruction arrangement is created in the 2nd floor as shown in Fig. 24. The bumper, if replaced with a spring, could replicate breathing mechanism if the spring at damage location in combination with stiffness of bumper spring provides total stiffness value equivalent to the stiffness of spring at undamaged position.

## Conclusion

The review in this article is developed considering the nonlinear behavior of a crack. Small damage of negligible severity may sometime impart nonlinearity in the system response under operating condition. Various nonlinear system identification techniques have already been developed in the past for different purposes. Those methods can be applied for structural damage detection when

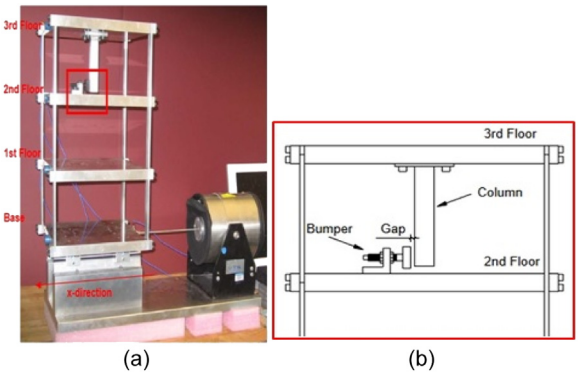


**Fig. 24.** (a) Three story frame building model attached with dynamic shaker, and (b) enlarged view of displacement restraining arrangement on the top floor [100].

the crack is too small to detect by existing methods and exhibits breathing mechanism during vibration. The study on the identification of the opening and closing mechanism of cracks is extensively used in the field of mechanical and electrical engineering. Recognizing the future prospect of nonlinear behavior of crack in the wide field of engineering, an extensive review on breathing crack is performed in this work. For the first time, a review on each step related to the identification of breathing crack in a structure and its modeling to simulate real behavior is summarized in a single article. It will facilitate researchers in building a complete comprehensive idea about breathing crack related problems. The fundamentals of closing crack is first explained with detailed mathematical background visualizing the actual behavior of the crack during vibration. It is then extended to review different nonlinear system identification techniques which are directly employed for the identification of breathing crack. Difficulties in the identification of nonlinearity lie in the solution of nonlinear equations. The methods for identification of breathing crack in this review are classified into two groups; vibration based methods and acoustic based methods. Volterra series is considered as the foundation of most expansion series based techniques used to identify system behavior. It is first expressed in time domain by applying convolution integral technique of linear system. Later, to easily identify kernel function of higher order Volterra series, FFT is applied to evaluate the function in the frequency domain. A connection is also established mathematically between Volterra series and other expansion series employed for system identification in the frequency domain. Further, the performances are highlighted with the advantages and limitations of vibration and acoustic based methods.

Modeling a cracked member is an integral part of the systematic application of structural health monitoring. The efficiency of any formulation can be judged only if the numerical model is precisely developed to simulate a breathing crack. Software packages that are popularly used in earlier studies are mentioned here with a detailed description of crack modeling in those environments. It helps either to develop a new model with improved accuracy or to validate a proposed method. The application of any formulation on large-scale structures first necessitates its verification on a simplified small-scale experimental model. Simulation of real practical scenarios in the controlled environment of the laboratory is a complicated task. It requires minute details about the real system parameters and their behavior under dynamic motion. Keeping in view this aspect, some of the experimentations successfully performed in the past are depicted here with detailed material properties and required parameters. It will minimize the efforts required to design a system with the real behavior of crack. It is also reviewed that experimental models designed for nonlinear system identification with an arrangement for impact nonlinearity can also be used for the simulation of breathing crack mechanism with necessary modifications.

Throughout the work, a wide range of techniques are incorporated to fulfill the aim of this article. Considering a vast range of available techniques in nonlinear dynamics and acoustics, some of the methods in each category are excluded from this extensive study for the brevity of article. A detailed discussion on Bayesian approach, wavelet transform method, etc. are kept out of scope in the present study. The future scopes obtained from this review are enumerated below:

(a) Nonlinear behavior of fatigue crack has been identified by different methods in the past. However, various other sources of nonlinearity may exist to pollute the response of already distorted signals. Hence, a robust technique should be developed to isolate different types of nonlinearity.
(b) Most of the breathing crack detection techniques are validated with numerical techniques or small scale experimental model of plate, beam, and rotor etc. An extensive study with a more complicated structure or real data is required.
(c) Application of most of the techniques for the determination of higher-order harmonics is either time-consuming or prone to erroneous results. A simple and efficient solution for the detection of higher harmonics in the response of any nonlinear system can be developed in the future.
(d) The physical reason behind the formation of only integer multiple of harmonics in the presence of nonlinearity is not properly explained yet. Extensive research needs to be performed to understand the physical behavior of nonlinear systems.
(e) A very few indicators evolved in the past monotonically varied in presence of nonlinearity and are independent of excitation parameters. It is a limitation for the quantification study of a nonlinear crack model. A bounded solution for the quantification of breathing crack is to be focused in future.

(f) A highly nonlinear system often leads to chaotic motion. Robust solution procedure to forecast this dynamically chaotic system rarely exists. The development of a general solution to describe both weak and strong nonlinear systems is one of the scopes of future research.

## Ethics statements

The Author had followed MethodsX ethical guidelines, this work does not involve human subjects, animal experiments or data collected from social media.

## CRediT author statement

Sayandip Ganguly is the sole author and responsible for all elements of this paper.

## Declaration of Competing Interest

The author declares that he has no known competing financial interests or personal relationships that could have appeared to influence the work reported in this paper.

## Data availability

No data was used for the research described in the article.

## Acknowledgments

The author would like to thank Dr. Koushik Roy (Assistant Professor, Department of Civil and Environmental Engineering, IIT Patna, India) for his valuable guidance and inspiration in writing this comprehensive review. The assistance received from the Department of Civil and Environmental Engineering, IIT Patna, in preparing this review.

## References

[1] M.M.A. Wahab, G.D. Roeck, Damage detection in bridges using modal curvatures: application to a real damage scenario, J. Sound Vib. 226 (2) (1999) 217–235.
[2] F. Zaker, E. Mueller, Investigation of a Columbus, Ohio train derailment caused by fractured rail, Case Stud. Eng. Fail. Anal. 7 (2016) 41–49.
[3] Y.F. Lee, Y. Lu, Identification of fatigue crack under vibration by nonlinear guided waves, Mech. Syst. Signal Process 163 (2022) 108138.
[4] P.G. Kirmsher, The effect of discontinuities on the natural frequency of beams, 44 (1944) 897–904.
[5] A.D. Dimarogonas, Vibration of cracked structures: a state of the art review, Eng. Fract. Mech. 55 (5) (1996) 831–857.
[6] T. Pafelias, Dynamic behaviour of a cracked rotor. general electric co., technical information series, no, Tech. Rep., 1974.
[7] O. Buck, W.L. Morris, J.M. Richardson, Acoustic harmonic generation at unbonded interfaces and fatigue cracks, Appl. Phys. Lett. 33 (5) (1978) 371–373.
[8] S.L. Tsyfansky, V.I. Beresnevich, Non-linear vibration method for detection of fatigue cracks in aircraft wings, J. Sound Vib. 236 (1) (2000) 49–60.
[9] S. Maezawa, H. Kumano, Y. Minakuchi, Forced vibrations in an unsymmetric piecewise-linear system excited by general periodic force functions, Bull. JSME 23 (175) (1980) 68–75.
[10] H. Kumano, S. Maezawa, Forced vibrations in an unsymmetric piecewise-linear system excited by general periodic force functions: 2nd report, the analysis up to the 4th order superharmonic resonance by means of the method of convergency improvement, Bull. JSME 25 (206) (1982) 1289–1298.
[11] S. Saito, Calculation of nonlinear unbalance response of horizontal Jeffcott rotors supported by ball bearings with radial clearances, J. Vib. Acoust. Stress Reliab. Des. 107 (4) (1985) 416–420.
[12] Y.S. Choi, S.T. Noah, Forced periodic vibration of unsymmetric piecewise-linear systems, J. Sound Vib. 121 (1) (1988) 117–126.
[13] R. Clark, W.D. Dover, L.J. Bond, The effect of crack closure on the reliability of NDT predictions of crack size, NDT Int. 20 (5) (1987) 269–275.
[14] S.L. Tsyfanskii, M.A. Magone, V.M. Ozhiganov, Using nonlinear effects to detect cracks in the rod elements of structures, Soviet J. Nondestructive Testing-Ussr 21 (3) (1985) 224–229.
[15] M.H.H. Shen, Y. Chu, Vibrations of beams with a fatigue crack, Comput. Struct. 45 (1) (1992) 79–93.
[16] M. Karthikeyan, R. Tiwari, S. Talukdar, Crack localisation and sizing in a beam based on the free and forced response measurements, Mech. Syst. Signal Process 21 (3) (2007) 1362–1385.
[17] Y.C. Chu, M.H.H. Shen, Analysis of forced bilinear oscillators and the application to cracked beam dynamics, Am. Inst. Aeronaut. Astronaut. 30 (10) (1992) 2512–2519.
[18] A.W. Davies, T.M. Roberts, Numerical studies of fatigue induced by breathing of slender web plates, Thin Walled Struct. 25 (4) (1996) 319–333.
[19] R. Ruotolo, C. Surace, P. Crespo, D. Storer, Harmonic analysis of the vibrations of a cantilevered beam with a closing crack, Comput. Struct. 61 (6) (1996) 1057–1074.
[20] T.G. Chondros, A.D. Dimarogonas, J. Yao, Vibration of a beam with a breathing crack, J. Sound Vib. 239 (1) (2001) 57–67.
[21] G. Kerschen, K. Worden, A.F. Vakakis, J.C. Golinval, Past, present and future of nonlinear system identification in structural dynamics, Mech. Syst. Signal Process 20 (3) (2006) 505–592.
[22] Z.K. Peng, Z.Q. Lang, S.A. Billings, Crack detection using nonlinear output frequency response functions, J. Sound Vib. 301 (3–5) (2007) 777–788.
[23] A. Chatterjee, Structural damage assessment in a cantilever beam with a breathing crack using higher order frequency response functions, J. Sound Vib. 329 (16) (2010) 3325–3334.
[24] M. Rezaee, R. Hassannejad, A new approach to free vibration analysis of a beam with a breathing crack based on mechanical energy balance method, Acta Mech. Solida Sin. 24 (2) (2011) 185–194.
[25] G. Yan, A.D. Stefano, E. Matta, R. Feng, A novel approach to detecting breathing-fatigue cracks based on dynamic characteristics, J. Sound Vib. 332 (2) (2013) 407–422.
[26] L. Chen, J. Xue, Z. Zhang, W. Zhang, Bifurcation study of thin plate with an all-over breathing crack, Adv. Mater. Sci. Eng. 2016 (2016).
[27] Y.H. Huang, J. Chen, W. Ge, X. Bian, W.H. Hu, Research on geometric features of phase diagram and crack identification of cantilever beam with breathing crack, Results Phys. 15 (2019) 102561.
[28] J.M. Richardson, Harmonic generation at an unbonded interface-I. planar interface between semi-infinite elastic media, Int. J. Eng. Sci. 17 (1) (1979) 73–85.
[29] Q. Shan, R.J. Dewhurst, Surface-breaking fatigue crack detection using laser ultrasound, Appl. Phys. Lett. 62 (21) (1993) 2649–2651.
[30] I.Y. Solodov, N. Krohn, G. Busse, CAN: an example of nonclassical acoustic nonlinearity in solids, Ultrasonics 40 (2002) 621–625.

[31] H. Cho, C. Lissenden, Structural health monitoring of fatigue crack growth in plate structures with ultrasonic guided waves, Struct. Health Monit. 11 (4) (2012) 393–404.
[32] Y. Shen, V. Giurgiutiu, Predictive modeling of nonlinear wave propagation for structural health monitoring with piezoelectric wafer active sensors, J. Intell. Mater. Syst. Struct. 25 (4) (2014) 506–520.
[33] K. Wang, M. Liu, Z. Su, S. Yuan, Z. Fan, Analytical insight into “breathing” crack-induced acoustic nonlinearity with an application to quantitative evaluation of contact cracks, Ultrasonics 88 (2018) 157–167.
[34] K. Wang, Z. Su, S. Yuan, Evaluation of crack orientation using fatigue crack-induced contact acoustic nonlinearity, Health Monit. Struct. Biol. Syst. XII 10600 (2018) 78–88.
[35] Y. Shen, C.E.S. Cesnik, Nonlinear scattering and mode conversion of lamb waves at breathing cracks: an efficient numerical approach, Ultrasonics 94 (2019) 202–217.
[36] L. Xu, K. Wang, X. Yang, Y. Su, J. Yang, Y. Liao, P. Zhou, Z. Su, Model-driven fatigue crack characterization and growth prediction: a two-step, 3-D fatigue damage modeling framework for structural health monitoring, Int. J. Mech. Sci. 195 (2021) 106226.
[37] L. Xu, Y. Su, K. Wang, X. Yang, S. Yuan, Z. Su, An elastodynamic reciprocity theorem-based closed-form solution to second harmonic generation of lamb waves by a fatigue crack: theory & experimental validation, J. Sound Vib. 509 (2021) 116226.
[38] L. Xu, K. Wang, Y. Su, Y. He, J. Yang, S. Yuan, Z. Su, Surface/sub-surface crack-scattered nonlinear rayleigh waves: a full analytical solution based on elasto-dynamic reciprocity theorem, Ultrasonics 118 (2022) 106578.
[39] K. Worden, C.R. Farrar, J. Haywood, M. Todd, A review of nonlinear dynamics applications to structural health monitoring, Struct. Control Health Monit. 15 (4) (2008) 540–567.
[40] D. Broda, W.J. Staszewski, A. Martowicz, T. Todd, Modelling of nonlinear crack–wave interactions for damage detection based on ultrasound—a review, J. Sound Vib. 333 (4) (2014) 1097–1118.
[41] H.H. Khodaparast, H. Madinei, M.I. Friswell, S. Adhikari, S. Coggon, J.E. Cooper, An extended harmonic balance method based on incremental nonlinear control parameters, Mech. Syst. Signal Process 85 (2017) 716–729.
[42] P. Gudmundson, The dynamic behaviour of slender structures with cross-sectional cracks, J. Mech. Phys. Solids 31 (4) (1983) 329–345.
[43] C.M. Cheng, Z.K. Peng, W.M. Zhang, G. Meng, Volterra-series-based nonlinear system modeling and its engineering applications: a state-of-the-art review, Mech Syst Signal Process 87 (2017) 340–364.
[44] R.M. Lin, T.Y. Ng, A new method for the accurate measurement of higher-order frequency response functions of nonlinear structural systems, ISA Trans. 81 (2018) 270–285.
[45] Z. Lang, S.A. Billings, Energy transfer properties of non-linear systems in the frequency domain, Int. J. Control 78 (2005) 345–362.
[46] C.M. Cheng, Z.K. Peng, X.J. Dong, W.M. Zhang, G. Meng, Locating non-linear components in two dimensional periodic structures based on NOFRFs, Int. J. Non Linear Mech. 67 (2014) 198–208.
[47] J.A.V. Feijoo, K. Worden, R. Stanway, Associated linear equations for Volterra operators, Mech. Syst. Signal Process 19 (1) (2005) 57–69.
[48] S. Roy, T. Bose, K. Debnath, Detection of local defect resonance frequencies using bicoherence analysis, J. Sound Vib. 443 (2019) 703–716.
[49] M. Jiang, D. Wang, Y. Kuang, X. Mo, A bicoherence-based nonlinearity measurement method for identifying the location of breathing cracks in blades, Int. J. Non Linear Mech. 135 (2021) 103751.
[50] M.A.A.S. Choudhury, D.S. Shook, S.L. Shah, Linear or nonlinear? a bicoherence based metric of nonlinearity measure, in: Proceedings of 6th IFAC Symposium on Fault Detection, Supervision and Safety of Technical Processes, 39, 2006, pp. 617–622.
[51] J.W.A. Fackrell, P.R. White, J.K. Hammond, R.J. Pinnington, A.T. Parsons, The interpretation of the bispectra of vibration signals-: I. theory, Mech. Syst. Signal Process 9 (3) (1995) 257–266.
[52] J.K. Sinha, Higher order coherences for fatigue crack detection, Eng. Struct. 31 (2) (2019) 534–538.
[53] Z.K. Peng, Z. Lang, S. Billings, G. Tomlinson, Comparisons between harmonic balance and nonlinear output frequency response function in nonlinear system analysis, J. Sound Vib. 311 (1) (2008) 56–73.
[54] A.H. Nayfeh, Introduction to Perturbation Techniques, John Wiley & Sons, 2011.
[55] J.H. He, Homotopy perturbation method: a new nonlinear analytical technique, Appl. Math. Comput. 135 (2003) 73–79.
[56] M. Azad, M.S. Alam, M.S. Rahman, B.S. Sarker, A general multiple-time-scale method for solving an n-th order weakly nonlinear differential equation with damping, Commun. Korean Math. Soc. 26 (4) (2011) 695–708.
[57] C.S. Liu, Y.W. Chen, A simplified Lindstedt-Poincaré method for saving computational cost to determine higher order nonlinear free vibrations, Mathematics 9 (23) (2021) 3070.
[58] X.J. Dong, Z.K. Peng, W.M. Zhang, G. Meng, Connection between Volterra series and perturbation method in nonlinear systems analyses, Acta Mech. Sin. 30 (4) (2014) 600–606.
[59] H. Long, Y. Liu, K. Liu, Nonlinear vibration analysis of a beam with a breathing crack, Appl. Sci. 9 (18) (2019) 3874.
[60] W. Wang, J. Cao, D. Mallick, S. Roy, J. Lin, Comparison of harmonic balance and multi-scale method in characterizing the response of monostable energy harvesters, Mech. Syst. Signal Process 108 (2018) 252–261.
[61] J. Prawin, K. Lakshmi, A.R.M. Rao, A novel vibration based breathing crack localization technique using a single sensor measurement, Mech. Syst. Signal Process 122 (2019) 117–138.
[62] J. Prawin, A.R.M. Rao, Vibration-based breathing crack identification using non-linear intermodulation components under noisy environment, Struct. Health Monit. 19 (1) (2020) 86–104.
[63] P. Liu, Damage detection using sideband peak count in spectral correlation domain, J. Sound Vib. 411 (2017) 20–33.
[64] A. Rytter, Vibrational based inspection of civil engineering structures, 1993.
[65] A. Nandi, S. Neogy, Modelling of a beam with a breathing edge crack and some observations for crack detection, J. Vib. Control 8 (5) (2002) 673–693.
[66] M. Cao, Q. Lu, Z. Su, M. Radzienski, W. Xu, W. Ostachowicz, A nonlinearity-sensitive approach for detection of “breathing” cracks relying on energy modulation effect, J. Sound Vib. 524 (2022) 116754.
[67] J.K. Sinha, M. Friswell, S. Edwards, Simplified models for the location of cracks in beam structures using measured vibration data, J. Sound Vib. 251 (1) (2002) 13–38.
[68] M. Hong, Z. Su, Q. Wang, L. Cheng, X. Qing, Modeling nonlinearities of ultrasonic waves for fatigue damage characterization: theory, simulation, and experimental validation, Ultrasonics 54 (3) (2014) 770–778.
[69] R. Apalowo, D. Chronopoulos, S.C. Chinchilla, Wave interaction with nonlinear damage and generation of harmonics in composite structures, Compos. Struct. 230 (2019) 111495.
[70] P.B. Negy, Fatigue damage assessment by nonlinear ultrasonic materials characterization, Ultrasonics 36 (1–5) (1998) 375–381.
[71] M. Hayes, R.S. Rivlin, Surface waves in deformed elastic materials, Arch. Ration. Mech. Anal. 8 (1961) 358–380.
[72] K. Kawashima, R. Omote, T. Ito, H. Fujita, T. Shima, Nonlinear acoustic response through minute surface cracks: FEM simulation and experimentation, Ultrasonics 40 (1–8) (2002) 611–615.
[73] M. Yuan, J. Zhang, S.J. Song, H.J. Kim, Numerical simulation of Rayleigh wave interaction with surface closed cracks under external pressure, Wave Motion 57 (2015) 143–153.
[74] P. Cawley, D. Alleyne, The use of Lamb waves for the long range inspection of large structures, Ultrasonics 34 (2–5) (1996) 287–290.
[75] M. Deng, Analysis of second-harmonic generation of Lamb modes using a modal analysis approach, J. Appl. Phys. 94 (6) (2003) 4152–4159.
[76] M. Deng, P. Wang, X. Lv, Experimental observation of cumulative second-harmonic generation of Lamb-wave propagation in an elastic plate, J. Phys. D Appl. Phys. 38 (2) (2005) 344.
[77] Y. Zhao, F. Li, P. Cao, Y. Liu, J. Zhang, S. Fu, J. Zhang, N. Hu, Generation mechanism of nonlinear ultrasonic Lamb waves in thin plates with randomly distributed micro-cracks, Ultrasonics 79 (2017) 60–67.

[78] T. Kundu, K. Wang, Z. Su, Analytical modeling of contact acoustic nonlinearity of guided waves and its application to evaluating severity of fatigue damage, Health Monit. Struct. Biol. Syst. 9805 (2016) 155–167.
[79] J. Jingpin, M. Xiangji, H. Cunfu, W. Bin, Nonlinear Lamb wave-mixing technique for micro-crack detection in plates, NDT E Int. 85 (2017) 63–71.
[80] D.M. Donskoy, A.M. Sutin, Vibro-acoustic modulation nondestructive evaluation technique, J. Intell. Mater. Syst. Struct. 9 (9) (1998) 765–771.
[81] M. Meo, G. Zumpano, Nonlinear elastic wave spectroscopy identification of impact damage on a sandwich plate, Compos. Struct. 71 (3–4) (2005) 469–474.
[82] A. Klepka, W.J. Staszewski, R.B. Jenal, M. Szwedo, J. Iwaniec, T. Uhl, Nonlinear acoustics for fatigue crack detection–experimental investigations of vibro-acoustic wave modulations, Struct. Health Monit. 11 (2) (2012) 197–211.
[83] Y. He, Y. Xiao, Z. Su, Y. Pan, Z. Zhang, Contact acoustic nonlinearity effect on the vibro-acoustic modulation of delaminated composite structures, Mech. Syst. Signal Process 163 (2022) 108161.
[84] S. Sikdar, P. Fiborek, P. Kudela, S. Banerjee, W. Ostachowicz, Effects of debonding on Lamb wave propagation in a bonded composite structure under variable temperature conditions, Smart Mater. Struct. 28 (1) (2018) 015021.
[85] R. Gorgin, Y. Luo, Z. Wu, Environmental and operational conditions effects on Lamb wave based structural health monitoring systems: a review, Ultrasonics 105 (2020) 106114.
[86] R. Gasch, A survey of the dynamic behaviour of a simple rotating shaft with a transverse crack, J. Sound Vib. 160 (2) (1993) 313–332.
[87] I.W. Mayes, W.G.R. Davies, Analysis of the response of a multi-rotor-bearing system containing a transverse crack in a rotor, J. Vib. Acoust. Stress Reliab. Des. 106 (1) (1984) 139–145.
[88] J. Penny, M. Friswell, Simplified modelling of rotor cracks, Key Eng. Mater. 245-246 (2003) 223–232.
[89] O.S. Jun, H.J. Eun, Y.Y. Earmme, C.W. Lee, Modelling and vibration analysis of a simple rotor with a breathing crack, J. Sound Vib. 155 (2) (1992) 273–290.
[90] C. Wei, X. Shang, Analysis on nonlinear vibration of breathing cracked beam, J. Sound Vib. 461 (2019) 114901.
[91] D.M. Joglekar, M. Mitra, Analysis of flexural wave propagation through beams with a breathing crack using wavelet spectral finite element method, Mech. Syst. Signal Process 76-77 (2016) 576–591.
[92] K.V. Nguyen, Comparison studies of open and breathing crack detections of a beam-like bridge subjected to a moving vehicle, Eng. Struct. 51 (2013) 306–314.
[93] M. Cao, Z. Su, T. Deng, W. Xu, Nonlinear pseudo-force in “breathing” delamination to generate harmonics: a mechanism and application study, Int. J. Mech. Sci. 192 (2021) 106124.
[94] F.E. Dotti, V.H. Cortnez, F. Reguera, Non-linear dynamic response to simple harmonic excitation of a thin-walled beam with a breathing crack, Áppl. Math. Model. 40 (1) (2016) 451–467.
[95] R. Courant, K. Friedrichs, H. Lewy, On the partial difference equations of mathematical physics, IBM J. Res. Dev. 11 (2) (1967) 215–234.
[96] W. Xu, Z. Su, M. Radzienski, M. Cao, W. Ostachowicz, Nonlinear pseudo-force in a breathing crack to generate harmonics, J. Sound Vib. 492 (2021) 115734.
[97] S. Cui, P. Maghoul, X. Liang, N. Wu, Q. Wang, Structural fatigue crack localisation based on spatially distributed entropy and wavelet transform, Eng. Struct. 266 (2022) 114544.
[98] M. Rébillat, R. Hajrya, N. Mechbal, Nonlinear structural damage detection based on cascade of hammerstein models, Mech. Syst. Signal Process 48 (1–2) (2014) 247–259.
[99] X. Kong, J. Li, Non-contact fatigue crack detection in civil infrastructure through image overlapping and crack breathing sensing, Autom. Constr. 99 (2019) 125–139.
[100] C.R. Farrar, M. Todd, E. Vigil, [Online]. Available: https://www.lanl.gov/projects/national-security-education-center/engineering/ei-software-download/index.php. (accessed 1st January 2023)